

GEOMETRIC REALIZATIONS OF THE MULTIPLIHEDRON AND ITS COMPLEXIFICATION.

S. MAU AND C. WOODWARD

ABSTRACT. We realize Stasheff's multiplihedron geometrically as the moduli space of stable quilted disks. This generalizes the geometric realization of the associahedron as the moduli space of stable disks. We also construct an algebraic variety that has the multiplihedron as its non-negative real part, and use it to define a notion of morphism of cohomological field theories.

CONTENTS

Introduction	2
Part 1. The associahedron, nodal disks, and metric trees.	6
1.1. The associahedron.	6
1.2. Moduli of semistable nodal disks	7
1.3. Metric ribbon trees	16
1.4. Toric varieties and moment polytopes.	20
Part 2. The multiplihedron, quilted disks, and bicolored metric trees.	24
2.1. The multiplihedron.	24
2.2. Moduli spaces of quilted disks	26
2.3. Bicolored metric ribbon trees.	35
2.4. Toric varieties and moment polytopes.	40
Part 3. Stable scaled curves and morphisms of CohFT's	43
3.1. Moduli space of stable scaled lines.	43
3.2. Morphisms of Cohomological Field Theories	48
References	50

INTRODUCTION

The Stasheff polytopes, a.k.a. *associahedra*, have had many incarnations since their original appearance in Stasheff’s work on homotopy associativity [13] in the early 1960s. A particular realization of the associahedra as the compactified moduli space of nodal disk with markings is described by Fukaya and Oh in [4]. The natural cell decomposition arising from this compactification is dual to the cell decomposition arising from the compactification of a space of metric ribbon trees, which were originally introduced by Boardman and Vogt [1]. In this paper we describe analogous constructions for a related family of Stasheff polytopes, called the *multiplihedra*, which appear when defining A_∞ maps between A_∞ spaces, and whose combinatorics were described by Iwase and Mimura in [6]. We show that the multiplihedron is realized as the compactification of a moduli space of marked *quilted* disks, which are marked disks with one interior circle. There is a dual cell decomposition that comes from the compactification of a space of *bicolored* metric ribbon trees. We also show how the realizations of the associahedra and the multiplihedra as moduli of disks are homomorphic, via moment maps of certain projective toric varieties, to the convex hull realizations of the associahedra by Loday [8], and of the multiplihedra by Forcey [2]. We thank Diane Maclagan for originally suggesting a connection with toric varieties.

We note that a sequence of cell complexes closely related to the multiplihedra appears in [3]. The authors of [3] denote them by \mathcal{N}_{k+1} for $k = 1, 2, \dots$ and use them to define A_∞ maps. The geometric description of \mathcal{N}_{k+1} is similar to the space of quilted disks, in that it is a moduli space of stable marked nodal disks with some additional structure. The main difference is that their complex is a manifold (with boundary and corners), whereas the moduli space of quilted disks has toric singularities on its boundary.

The paper is divided into three parts. Part 1 is about the associahedron, and Part 2 is about the multiplihedron. We have used methods that generalize from Part 1 to Part 2, to make the analogies between the two cases clear. Part 3 is about a “complexification” of the multiplihedron. Here is an outline of the ideas used in each part.

Part 1. We begin with Stasheff’s original definition of the associahedron as a *CW*-complex, as in [13]. Then we introduce a moduli space \overline{M}_n of stable, $(n + 1)$ -marked nodal disks. \overline{M}_n is a compactification of the moduli space of disks with $(n + 1)$ *distinct* marked points on the boundary of the disk, which we denote by M_n .

We define a topology on \overline{M}_n by means of an embedding

$$\rho_d : \overline{M}_n \hookrightarrow [-\infty, 0]^N, \quad N = \binom{d+1}{4},$$

using cross-ratio coordinates, one for each subset of four marked points. This was done for $\overline{M}_{0,n}$ by McDuff and Salamon in [9, Appendix D], who showed moreover that the

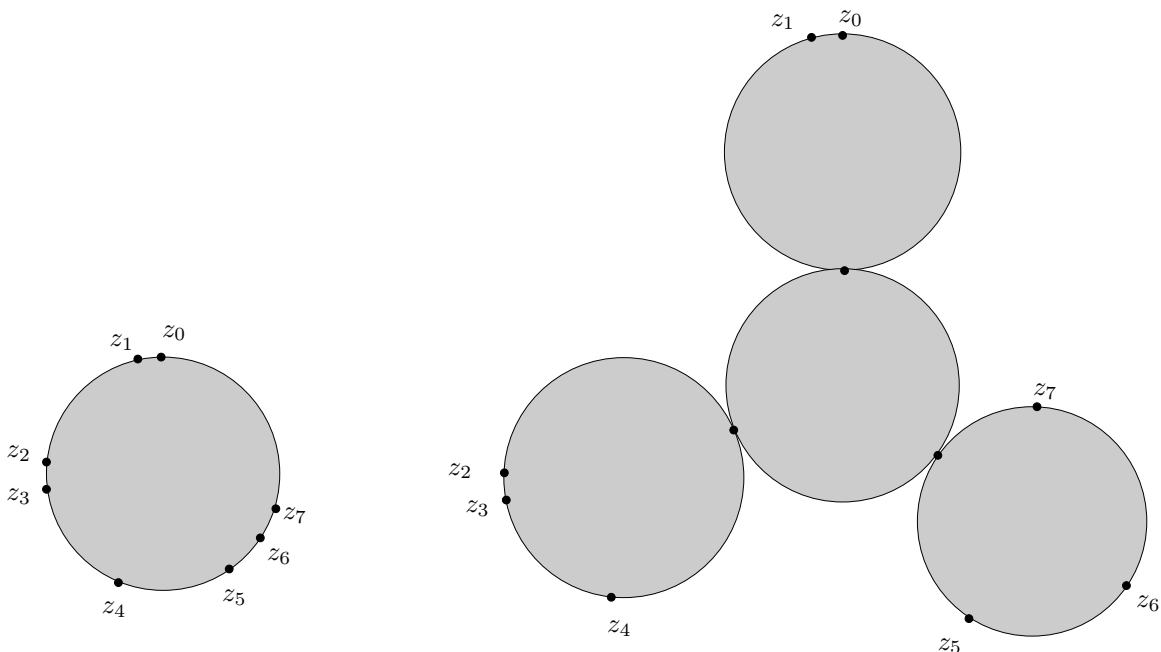


FIGURE 1. *Left:* a marked disk in M_7 . *Right:* a stable marked nodal disk in \overline{M}_7 .

extrinsic topology defined by this embedding coincides with the topology defined by Gromov convergence of stable maps, in the special case of the target manifold being a point. Following [9, Appendix D], we use the cross-ratios to define explicit charts for \overline{M}_n based on combinatorial types of the nodal disks. We then define an equivalent set of charts on \overline{M}_n , using coordinates that we have called “simple ratios” because the relations among them are much simpler. The simple ratios have a very natural description on M_n : for each disk with $n + 1$ distinct marked points on the boundary, choose a fractional linear transformation that sends the marked point z_0 to ∞ . The remaining marked points are all on the real axis of \mathbb{C} , still ordered $\infty < z_1 < z_2 < \dots < z_d < \infty$, and are completely determined up to dilation and translation, by the differences $z_{i+1} - z_i =: X_i$, for $i = 1, \dots, d - 1$. The differences X_i are translationally invariant, and the “simple ratios” are all ratios of the form X_i/X_j , which are invariant under dilations. Thus all simple ratios are well-defined on equivalence classes of marked disks, which are the elements of the moduli space.

We then introduce the moduli space of metric trees and show that they describe a dual decomposition of \overline{M}_n into cubes, a decomposition originally due to Boardman and Vogt. Finally, we identify \overline{M}_n with the non-negative part of a certain projective toric variety. The projective toric variety is constructed with weight vectors, using the algorithm given by Loday’s convex hull realization of the associahedron in [8]. It follows from the theory

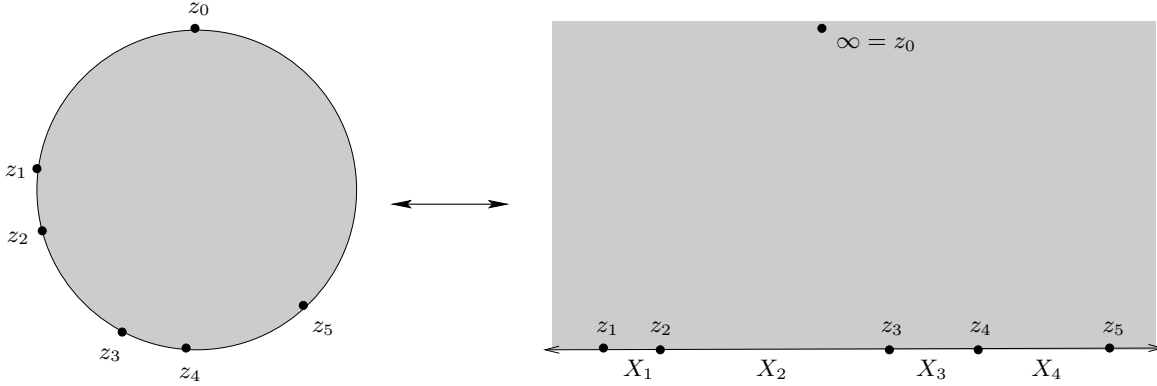


FIGURE 2. Defining the coordinates X_1, X_2, \dots, X_{d-1} .

of toric varieties that the moment map is a homeomorphism between the non-negative part of the variety and the moment polytope, which is the convex hull of the weights. This recovers the well-known fact that the moduli space \overline{M}_n is homeomorphic to the associahedron.

Part 2. We begin with the original inductive definition of the multiplihedron as a *CW* complex in [13], before introducing the moduli space $\overline{M}_{n,1}$ of stable, $(n+1)$ -marked, nodal quilted disks. This moduli space is a compactification of a moduli space $M_{n,1}$ of $(n+1)$ -marked quilted disks. A marked quilted disk has marked points z_0, z_1, \dots, z_n , on its boundary, and an inner circle which is tangent to z_0 . The group of orientation-preserving automorphisms of the disk acts on the marked quilted disks and the moduli space consists of the orbits of its action. By choosing a fractional linear transformation that sends the marked point z_0 to ∞ , and the interior of the disk to the upper half plane, an $(n+1)$ -marked quilted disk can be identified with the one point compactification of the upper half plane, with n marked points on the real axis, and a horizontal line L above the real axis. We define a topology on $\overline{M}_{n,1}$ by an embedding

$$\rho_{d1} \hookrightarrow [-\infty, 0]^N \times [0, \infty]^M, \quad N = \binom{d+1}{4}, \quad M = \binom{d}{2}$$

using two types of cross-ratio coordinate: a coordinate ρ_{ijkl} for each cyclically ordered subset $\{i, j, k, l\} \subset \{0, 1, \dots, d\}$ of size 4, and a coordinate $\rho_{i,j}$ for each pair $i < j$ in $\{1, 2, \dots, d\}$. The coordinate ρ_{ijkl} represents the image of z_l under the fractional linear transformation that sets $z_i = 0, z_j = 1$ and $z_k = \infty$. The cyclic order of i, j, k, l forces z_l to take a value in $[-\infty, 0]$. The other coordinate, $\rho_{i,j}$ corresponds to the height of the line L above the real axis with respect to a transformation setting $z_0 = \infty, z_i = 0$ and $z_j = 1$. The order $i < j$ forces L to lie in the upper half-plane, so its height is in $[0, \infty]$. We define charts for $\overline{M}_{n,1}$ using the cross-ratios, but in this case the chart coordinates carry relations, so the topology they define is not that of a manifold-with-corners, but of a

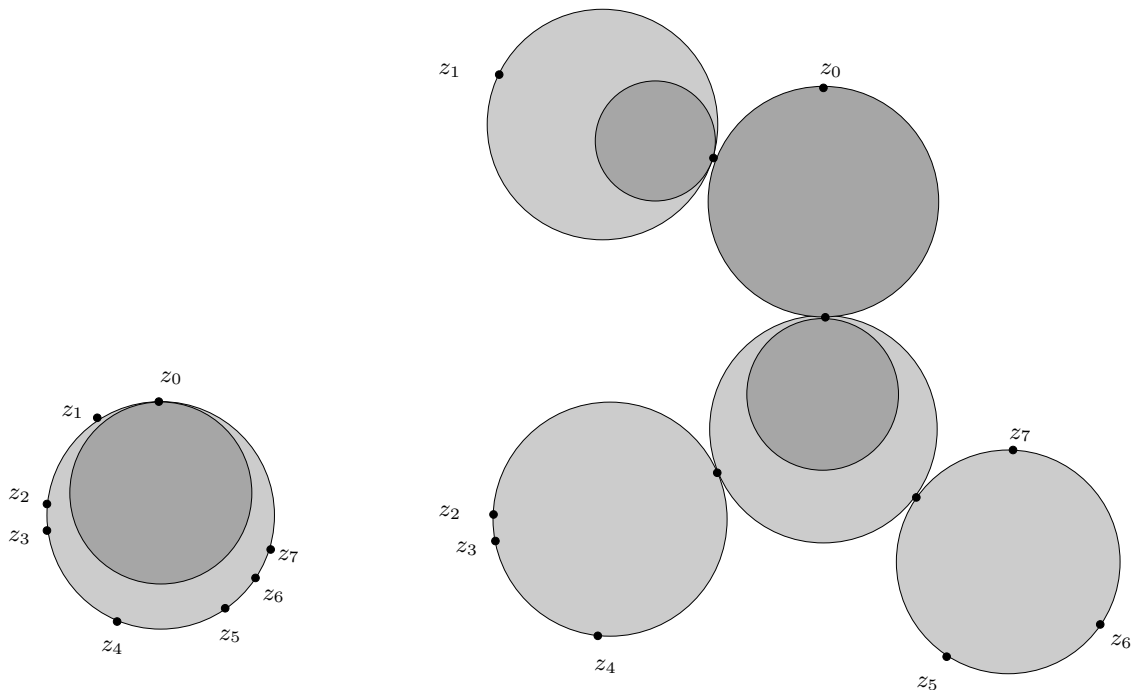
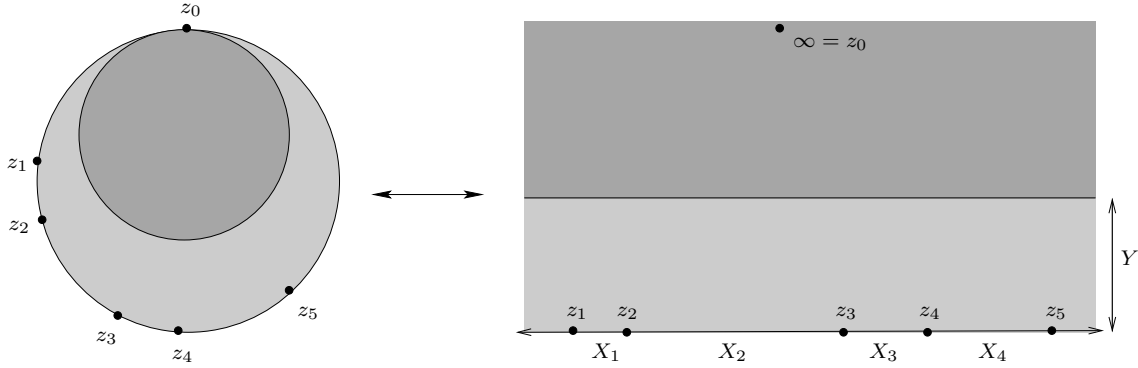


FIGURE 3. *Left:* A marked quilted disk in $M_{7,1}$. *Right:* A stable, nodal marked quilted disk in $\overline{M}_{7,1}$.

manifold with singularities, meaning that the local topology for points on the boundary is in general a polyhedral cone. As in Part 1, we replace the cross-ratio charts with equivalent charts that use only simple ratios. To get the simple ratios, use a fractional linear transformation that sends z_0 to ∞ . Define $X_i := z_{i+1} - z_i$, and define Y to be the height of the line L above the real axis. The quantities X_1, \dots, X_{d-1}, Y are all invariant under translation, and under dilations they scale simultaneously. The simple ratios are all ratios of the form X_i/X_j , Y/X_j or X_j/Y , which are well-defined as coordinates on the moduli space.

We then introduce a moduli space of bicolored metric trees, and show that they describe a dual decomposition of $\overline{M}_{n,1}$ into compactified polyhedral cones. We then construct a projective toric variety by means of weight vectors, and show that $\overline{M}_{n,1}$ fits into it as the non-negative part. The algorithm that we use for the weights is very closely related to the algorithm for the vertices of the multiplihedron in the convex hull construction of Forcey in [2]. The theory of toric varieties allows us to conclude that $\overline{M}_{n,1}$ is homeomorphic, via the moment map, to the convex hull of the weight vectors. Thus, $\overline{M}_{n,1}$ is homeomorphic to the multiplihedron.

FIGURE 4. Defining the coordinates X_1, \dots, X_{d-1}, Y .

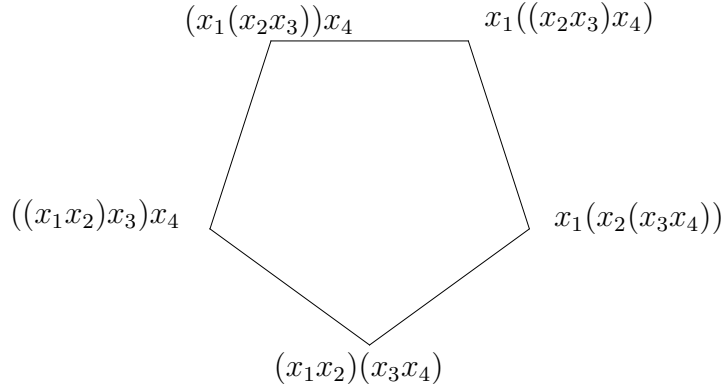
Part 3. We define a complex algebraic variety $\overline{M}_{n,1}^{\mathbb{C}}$ in which the moduli space of quilted disks sits as a component of the real locus. This is analogous to how the associahedron sits in a component of the real locus of the Deligne-Mumford space of genus zero stable nodal curves. The Deligne-Mumford spaces $\overline{DM}_{g,n}$ were used by Kontsevich and Manin in [7] to define Cohomological Field Theories (CohFTs). Here we use the spaces $\overline{M}_{n,1}^{\mathbb{C}}$ to propose a definition of *morphism* of CohFTs in the genus 0 case.

We thank Jim Stasheff for helpful comments and suggestions.

Part 1. The associahedron, nodal disks, and metric trees.

1.1. THE ASSOCIAHEDRON.

Let $d > 2$ be an integer. The d -th associahedron K_d is a CW -complex of dimension $d-2$ whose vertices correspond to the possible ways of parenthesizing d variables x_1, \dots, x_d .

FIGURE 5. Vertices of K_4

Each facet of K_d is the image of an embedding

$$(1) \quad \phi_{i,e} : K_i \times K_e \rightarrow K_d, \quad i + e = d + 1$$

corresponding to the expression $x_1 \dots x_{i-1}(x_i \dots x_{i+e})x_{i+e+1} \dots x_d$.

The associahedra are defined by induction as follows. Let K_3 be the closed unit interval. Let $d > 3$ and suppose that we have constructed the associahedra K_i for $i \leq d - 1$, together with the inclusions $K_i \times K_e \mapsto K_d$ corresponding to the facets of K_d . Stasheff defines

$$L_d = \bigcup (K_i \times K_e) / \sim$$

where the union is over the facets of K_d , and the equivalence relation \sim is defined by identifying the components in the image of the map

$$K_{i_1} \times K_{i_2} \times K_{i_3} \rightarrow (K_{i_1+i_2} \times K_{i_3}) \times (K_{i_1} \times K_{i_2+i_3}).$$

Define K_d to be the cone on L_d .

The faces of K_d also correspond to rooted trees with $d + 1$ -branches and at least three edges meeting each vertex.

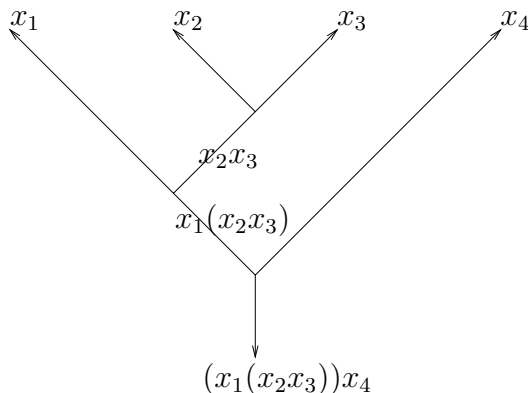


FIGURE 6. Tree corresponding to $(x_1(x_2x_3))x_4$

Alternatively the vertices correspond to triangulations of a regular $d + 1$ -gon. The edges of K_d correspond to changes of one bracketing, that is, changes of the tree by the move shown in Figure (7). The number of edges meeting any vertex is the number $d - 2$ of internal edges in the corresponding tree.

1.2. MODULI OF SEMISTABLE NODAL DISKS

A nodal disk D is obtained from a union of disks (called the components of D) by identifying points on the boundary. Any singular point is assumed to belong to exactly two disk components. The *combinatorial type* of the nodal disk is the graph (by assumption,

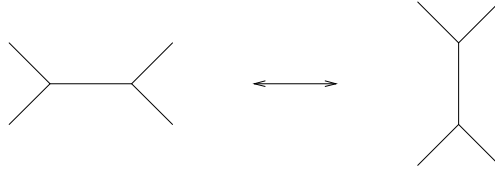
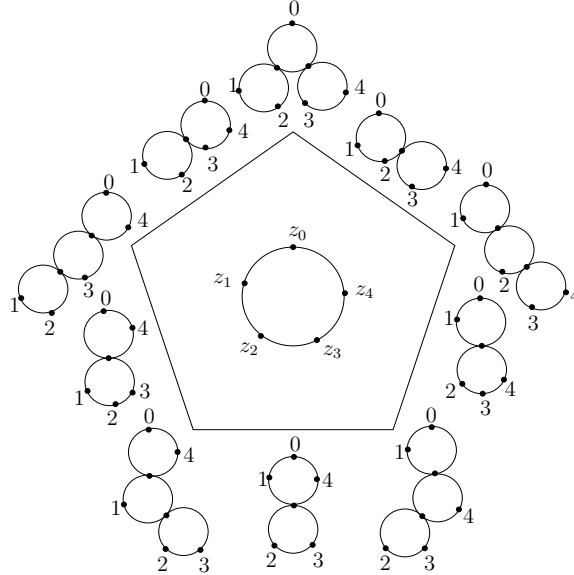


FIGURE 7. Move corresponding to an edge of the associahedron

a tree) obtained by replacing each disk with a vertex, and each singularity with an edge. A set of markings is a set $\{z_0, \dots, z_d\}$ of the boundary ∂D in clockwise order, distinct from the singularities. A nodal disk with markings is *semistable* if each disk component contains at least three singularities or markings. The combinatorial type of a nodal disks with markings is obtained from the graph above by adding semiinfinite edges associated to the markings. The resulting graph has a distinguished vertex defined by the component containing the zeroth marking z_0 . Thus the combinatorial type of a nodal disk with markings is a rooted tree. A morphism between nodal disks is a collection of holomorphic isomorphisms between the disk components, preserving the singularities and markings. Let $M_\Gamma(d)$ denote the set of isomorphism classes of semistable nodal marked disks of combinatorial type Γ , and

$$\overline{M}_d = \bigcup_{\Gamma} M_{d,\Gamma}.$$

The moduli space \overline{M}_4 is shown below in Figure 8.

FIGURE 8. \overline{M}_4 . Drawing all nodal disks with z_0 at the top makes the vertical axis of symmetry clear.

There is a canonical partial order on the combinatorial types, and we write $\Gamma' \leq \Gamma$ to mean that Γ' is obtained from Γ by contracting a subset of internal edges of Γ .

1.2.1. Topology via cross-ratios. In this section we introduce a topology on \overline{M}_d via cross-ratios, as in [9, Appendix D]. The cross-ratio of four distinct points $w_1, w_2, w_3, w_4 \in \mathbb{C}$ is

$$\rho_4(w_1, w_2, w_3, w_4) = \frac{(w_2 - w_3)(w_4 - w_1)}{(w_1 - w_2)(w_3 - w_4)}$$

and represents the image of w_4 under the fractional linear transformation that sends w_1 to 0, w_2 to 1, and w_3 to ∞ . ρ_4 is invariant under the action of $SL(2, \mathbb{C})$ on \mathbb{C} by fractional linear transformations. By identifying $\mathbb{P}^1 \rightarrow \mathbb{C} \cup \{\infty\}$ and using invariance we obtain an extension of ρ_4 to \mathbb{P}^1 , that is, a map

$$\rho_4 : \{(w_1, w_2, w_3, w_4) \in (\mathbb{P}^1)^4, \quad i \neq j \implies w_i \neq w_j\} \rightarrow \mathbb{C} - \{0\}.$$

ρ_4 naturally extends to the geometric invariant theory quotient

$$(\mathbb{P}^1)^4 // SL(2, \mathbb{C}) = \{(w_1, w_2, w_3, w_4), \text{ no more than two points equal}\} / SL(2, \mathbb{C})$$

by setting

$$(2) \quad \rho_4(w_1, w_2, w_3, w_4) = \left\{ \begin{array}{ll} 0 & \text{if } w_2 = w_3 \text{ or } w_1 = w_4 \\ 1 & \text{if } w_1 = w_3 \text{ or } w_2 = w_4 \\ \infty & \text{if } w_1 = w_2 \text{ or } w_3 = w_4 \end{array} \right\}$$

and defines an isomorphism

$$\rho_4 : (\mathbb{P}^1)^4 // SL(2, \mathbb{C}) \rightarrow \mathbb{P}^1.$$

Let $\mathbb{R}_+^4 \subset \mathbb{R}^4$ denote the subset of distinct points $(w_1, w_2, w_3, w_4) \in \mathbb{R}^4$ in cyclic order. The restriction of ρ_4 to \mathbb{R}_+^4 takes values in $(-\infty, 0)$ and is invariant under the action of $SL(2, \mathbb{R})$ by fractional linear transformations. Hence it descends to a map

$$(\mathbb{R}^4)_+ / SL(2, \mathbb{R}) \rightarrow (-\infty, 0).$$

Let D denote the unit disk, and identify $D \setminus \{-1\}$ with the half plane \mathbb{H} by $z \mapsto 1/(z+1)$. Using invariance one constructs an extension

$$\rho_4 : (\partial D)_+^4 / SL(2, \mathbb{R}) = M_4 \rightarrow (-\infty, 0)$$

where $(\partial D)_+^4$ is the set of distinct points on ∂D in counterclockwise cyclic order. ρ_4 admits an extension to \overline{M}_4 via (2) and so defines an isomorphism

$$\rho_4 : \overline{M}_4 \rightarrow [-\infty, 0].$$

For any distinct indices i, j, k, l the cross-ratio ρ_{ijkl} is the function

$$\rho_{ijkl} : M_d \rightarrow \mathbb{R}, \quad [w_0, \dots, w_d] \mapsto \rho_4(w_i, w_j, w_k, w_l).$$

We extend ρ_{ijkl} to \overline{M}_d as follows. Let $\Gamma(ijkl) \subset \Gamma$ be the subtree whose ending edges are the semiinfinite edges i, j, k, l . The subtree $\Gamma(ijkl)$ is one of the three following types: In the first resp. third case, we define

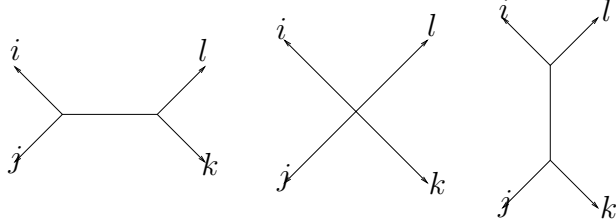


FIGURE 9. Cross-ratios by combinatorial type: for the first type, $\rho_{ijkl}(D) = -\infty$, for the second type $\rho_{ijkl}(D) \in (-\infty, 0)$, and for the third type $\rho_{ijkl}(D) = 0$.

$$\rho_{ijkl}(D) = -\infty \quad \text{resp. } 0.$$

In the second case, let $\overline{w}_i, \overline{w}_j, \overline{w}_k, \overline{w}_l$ be the points on the component where the four branches meet and define

$$\rho_{ijkl}(D) = \rho(\overline{w}_i, \overline{w}_j, \overline{w}_k, \overline{w}_l).$$

The collection of functions ρ_{ijkl} , $i < j < k < l$ defines a map of sets

$$\rho_d : \overline{M}_d \mapsto [-\infty, 0]^N$$

where $N = \binom{d+1}{4}$.

The combinatorial type Γ of a point $p \in \overline{M}_d$ can be read off from $\rho_d(p)$ as follows. Note that if Γ is a tree, then removing any finite edge e of Γ divides Γ , and in particular the set $\text{Edge}^\infty(\Gamma)$ of semiinfinite edges, into two components. The tree can be re-constructed from the set of such partitions of $\text{Edge}^\infty(\Gamma)$. If some cross-ratio $\rho_{ijkl}(D)$ is ∞ (resp. 0), the semiinfinite edges i, j, k, l can be separated into pairs i, j and k, l (resp. i, l and j, k) by removing an edge (Figure 9). Thus the combinatorial structure of D is determined by which cross-ratios are 0 or $-\infty$. The positions of the marked points on each component with at least 4 markings or singularities can be re-constructed from the cross-ratios. Hence ρ_d is injective and so the pull-back ρ_d of the topology on the target defines on \overline{M}_d the structure of a compact Hausdorff topological space.

Remark 1.2.1. The map $\rho_{ijkl} : \overline{M}_d \rightarrow \overline{M}_4 \cong [-\infty, 0]$ is a special case of a type of *forgetful morphism* considered by Knudsen. More generally, for any subset $I \subset \{0, \dots, n\}$ of size k we have a continuous map $\overline{M}_d \mapsto \overline{M}_k$ obtained by forgetting the positions of the markings z_i , $i \notin I$ and collapsing the unstable components. By definition the topology on \overline{M}_d is the one for which all forgetful morphisms are continuous, and $\overline{M}_4 \cong [-\infty, 0]$.

1.2.2. Properties of the cross-ratio coordinates. The coordinates ρ_{ijkl} have the following properties, which can be derived from elementary facts about cross-ratios. The list is lifted straight from [9, Appendix D], in which the proofs can be found.

(Invariance): For all $p \in \overline{M}_d$, and for all $\phi \in SL(2, \mathbb{R})$, $\rho_{ijkl}(\phi(p)) = \rho_{ijkl}(p)$.

(Symmetry): $\rho_{jikl} = \rho_{ijlk} = 1 - \rho_{ijkl}$, and $\rho_{ikjl} = \frac{\rho_{ijkl}}{\rho_{ijkl} - 1}$.

(Normalization): $\rho_{ijkl} = \begin{cases} \infty, & \text{if } i = j \text{ or } k = l, \\ 1, & \text{if } i = k \text{ or } j = l, \\ 0, & \text{if } i = l \text{ or } j = k. \end{cases}$

(Recursion): As long as the set $\{1, \infty, \rho_{ijkl}, \rho_{ijkm}\}$ contains three distinct numbers, then

$$(3) \quad \rho_{jklm} = \frac{\rho_{ijkm} - 1}{\rho_{ijkm} - \rho_{ijkl}}$$

for any five pairwise distinct integers $i, j, k, l, m \in \{0, 1, \dots, d\}$. There is an equivalent version of this formula that will sometimes be more convenient to use; and that is that as long as the set $\{0, \infty, \rho_{mijk}, \rho_{mijl}\}$ contains three distinct numbers, then

$$(4) \quad 1 - \rho_{jklm} = \frac{\rho_{mijk}}{\rho_{mijl}}$$

1.2.3. Charts using cross-ratios. The cross-ratios can be used to construct explicit coordinate charts which give \overline{M}_d the structure of a $(d - 2)$ dimensional manifold-with-corners. A chart around a point in $p \in \overline{M}_d$ is defined based on the combinatorial type Γ of p . If $|E|$ is the number of interior edges of Γ , the chart is a homeomorphism between $(-\infty, 0)^{d-2-|E|} \times (-\infty, 0]^{|E|}$ and the open subset

$$\overline{M}(\Gamma) := \bigcup_{\Gamma' \leq \Gamma} M_d(\Gamma')$$

i.e., all points in \overline{M}_d whose combinatorial type is obtained from Γ by contracting a subset of interior edges.

The method we use to construct charts using the cross-ratios is taken from [9, Appendix D], and we include their proof here for the sake of completeness. For a combinatorial type Γ , a chart consists of

- (a) $n_v - 3$ cross-ratios for each vertex $v \in \Gamma$ that represents a disk component with n_v special points (i.e., marked points or singular points).
- (b) a cross-ratio $\rho_{ijkl} = 0$ for each internal edge in $e \in \Gamma$, where i, j, k and l are such that $\rho_{ijkl} = 0$ for any combinatorial type modeled on that edge.

This gives a total of

$$\begin{aligned}
\sum_{v \in \text{Vert}(\Gamma)} (n_v - 3) + \# \text{Edge}(\Gamma) &= d + 1 + 2\# \text{Edge}(\Gamma) - 3\# \text{Vert}(\Gamma) + \# \text{Edge}(\Gamma) \\
&= d + 1 + 3(\# \text{Edge}(\Gamma) - \# \text{Vert}(\Gamma)) \\
&= d - 2
\end{aligned}$$

coordinates, since the number of edges in a tree is one less than the number of vertices.

Theorem 1.2.2 (Theorem D.5.1 in [9]). *Let $p \in \overline{M}_n$. Suppose p has combinatorial type Γ , and that $d - 2$ cross-ratios have been chosen as prescribed by (a), (b) above. Then, in the open set $\overline{M}(\Gamma)$, all cross-ratio coordinates are smooth functions of those in the chart. Hence \overline{M}_d is a smooth manifold-with-corners of real dimension $d - 2$.*

Proof. Fix a combinatorial type Γ with $d + 1$ leaves. To show that the $d - 2$ coordinates described above form a chart in a neighborhood of p , we proceed by induction on the number of edges $|E|$ of the combinatorial type Γ .

If $|E| = 0$, Γ is the corolla with single vertex and $d + 1$ leaves, corresponding to the equivalence classes of the unit disk D with $d + 1$ distinct marked points z_0, \dots, z_d on ∂D . The $d - 2$ cross-ratios

$$\{\rho_{0123}, \rho_{0124}, \dots, \rho_{012d}\}$$

form a chart, since an explicit formula for all other cross-ratios is

$$\rho_{ijkl} = \frac{(\rho_{012j} - \rho_{012k})(\rho_{012l} - \rho_{012i})}{(\rho_{012i} - \rho_{012j})(\rho_{012k} - \rho_{012l})}$$

with well-defined limits

$$\rho_{ijkl} = \begin{cases} \infty, & \text{if } i = j \text{ or } k = l, \\ 1, & \text{if } i = k \text{ or } j = l, \\ 0, & \text{if } i = l \text{ or } j = k. \end{cases}$$

So assume that the statement holds for all trees with strictly less than $|E|$ edges, and consider a combinatorial type Γ with $|E|$ edges. Fix an edge e joining vertices α and β . Removing the edge e splits Γ into two subtrees, one containing α and the other containing β . For each of these trees, put a semiinfinite edge where e was. Denote by Γ_A the tree containing α , and by Γ_B the one containing β . Relabeling indices if necessary we can assume that Γ_A has marked points $0, \dots, m + 1$, and Γ_B has marked points m, \dots, d . Let ρ_A be the set of cross-ratios with indices in $\{0, \dots, m, m + 1\}$, and let ρ_B be the set of cross-ratios with indices in $\{m, m + 1, \dots, d\}$. By the inductive hypothesis, all cross-ratios in ρ_A are smooth functions of the cross-ratios in a chart for Γ_A , and all cross-ratios in ρ_B are smooth functions of the cross-ratios in a chart for Γ_B . Fix the cross-ratio $\rho_{0,m,m+1,d} = \infty$ to represent the edge e . Note that $\rho_{0,m,m+1,d} = \infty$ for all combinatorial types containing the edge e . We need to show that the chart for Γ_A ,

the chart for Γ_B , and $\rho_{0,m,m+1,d}$ together form a chart for Γ . It suffices to show that all cross-ratios with some indices less than or equal to m and other indices greater than or equal to $m+1$ are smooth functions of cross-ratios in ρ_A , ρ_B , and $\rho_{0,m,m+1,d}$. There are really only two cases to prove, namely

- (a) ρ_{ijkl} where $i, j \leq m$ and $k, l \geq m+1$, and
- (b) ρ_{ijkl} where $i, j, k \leq m$ and $l \geq m+1$,

since the only other case, $i \leq m$ and $j, k, l \geq m+1$, is dual to the latter. Since $\rho_{m+1,i,j,l} = 0$, applying Recursion formula (3),

$$\rho_{i,j,k,l} = \frac{\rho_{m+1,i,j,l} - 1}{\rho_{m+1,i,j,l} - \rho_{m+1,i,j,k}},$$

shows that it is enough to show that $\rho_{m+1,i,j,l}$ and $\rho_{m+1,i,j,k}$ are smooth functions of the chart coordinates. Note that if $k \leq m$, then $\rho_{m+1,i,j,k} \in \rho_A$, so is a smooth function of the chart coordinates. Therefore we only need to show that for $l > m+1$, the cross-ratio $\rho_{m+1,i,j,l}$ is a smooth function of the chart coordinates. But we also have that $\rho_{m,m+1,l,i} = 0$, so that the Recursion formula (3) holds,

$$\rho_{m+1,l,i,j} = \frac{\rho_{m,m+1,l,j} - 1}{\rho_{m,m+1,l,j} - \rho_{m,m+1,l,i}}.$$

So it is enough to prove that for all $i < m$ and all $l > m+1$, the cross-ratio $\rho_{m,m+1,l,i}$ is a smooth function of the chart coordinates.

To show this, first note that $\rho_{m,m+1,d,0} = 0$ so again by (3),

$$\rho_{m+1,d,0,l} = \frac{\rho_{m,m+1,d,l} - 1}{\rho_{m,m+1,d,l} - \rho_{m,m+1,d,0}}$$

and since $\rho_{m,m+1,d,l} \in \rho_B$ for $l > m+1$ we conclude that $\rho_{m+1,d,0,l}$ is a smooth function of the chart coordinates.

Next, $\rho_{d,m,l,0} = 1$ so by the variation (5) of the Recursion formula,

$$\begin{aligned} 1 - \rho_{l,0,m+1,d} &= \frac{\rho_{d,m,l,0}}{\rho_{d,m,l,m+1}} \\ \implies \rho_{d,m,l,0} &= \rho_{d,m,l,m+1}(1 - \rho_{l,0,m+1,d}) \end{aligned}$$

showing that $\rho_{d,m,l,0}$ is a smooth function of the chart coordinates.

Again using $\rho_{d,m,l,0} = 1$ and (5),

$$\begin{aligned} 1 - \rho_{m,l,m+1,0} &= \frac{\rho_{0,d,m,l}}{\rho_{0,d,m,m+1}} \\ \implies \rho_{m,l,m+1,0} &= 1 - \frac{\rho_{0,d,m,l}}{\rho_{0,d,m,m+1}} \end{aligned}$$

Next, $\rho_{m,m+1,0,l} = 1$ so by (5)

$$\begin{aligned} 1 - \rho_{0,l,i,m} &= \frac{\rho_{m,m+1,0,l}}{\rho_{m,m+1,0,i}} \\ \implies \rho_{0,l,i,m} &= 1 - \frac{\rho_{m,m+1,0,l}}{\rho_{m,m+1,0,i}}. \end{aligned}$$

Finally, $\rho_{m,l,i,m+1} = 1$ implies, by (5) again,

$$\begin{aligned} 1 - \rho_{i,m+1,0,m} &= \frac{\rho_{m,l,i,m+1}}{\rho_{m,l,i,0}} \\ \implies \rho_{m,l,i,m+1} &= \rho_{m,l,i,0}(1 - \rho_{i,m+1,0,m}) \end{aligned}$$

proving that $\rho_{m,l,i,m+1}$ is a smooth function of the chart coordinates. □

Remark 1.2.3. The charts corresponding to maximal combinatorial types – that is, the binary trees – suffice to cover the whole moduli space, since all combinatorial types can be obtained from the maximal ones by contracting an edge. From now on we will think of each chart as being from a maximal tree. We can also assume that all cross-ratios in the chart are of the form ρ_{ijk0} or ρ_{0ijk} , since all edges in a binary tree can be given coordinates of that form. In other words, we can assume that all chart coordinates have been chosen relative to the root of the tree, where the root corresponds to the distinguished marked point z_0 .

1.2.4. Charts using simple ratios. Let T be a maximal tree representing a combinatorial type in \overline{M}_d . Each pair of adjacent leaves in T , i and $i+1$ say, determines a unique vertex which we label v_i . By choosing parametrizations such that $z_0 = \infty$, points in \overline{M}_d are configurations of d distinct points in \mathbb{R} ,

$$-\infty < z_1 < z_2 < \dots < z_d < \infty,$$

modulo translation and scaling. Set $X_i = z_{i+1} - z_i$. Each edge in T is determined by a pair of vertices, say v_i and v_j . If v_i is closer to the root of the tree than v_j , we give the edge the coordinate X_j/X_i .

Example 1.2.4. Figure 10 shows the two charts for a combinatorial type in \overline{M}_6 .

1.2.5. Equivalence of charts. Each cross-ratio in a chart is a smooth function of the simple ratios, and is zero if and only if the corresponding simple ratio for that edge is zero. The vice-versa is also true, and the proof is much the same. By symmetry it suffices to consider the edge pictured in Figure 11, where an edge joins vertices v_r and v_s , and v_r is above v_s , and the cross-ratio allocated to the edge is ρ_{ijk0} . Parametrizing

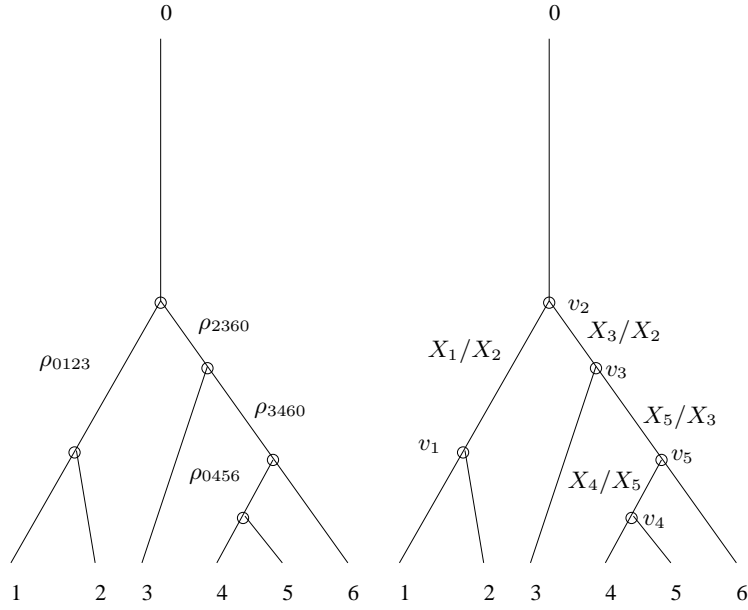


FIGURE 10. Two equivalent charts, one using cross-ratios and the other using simple ratios, for a combinatorial type in \overline{M}_6 .

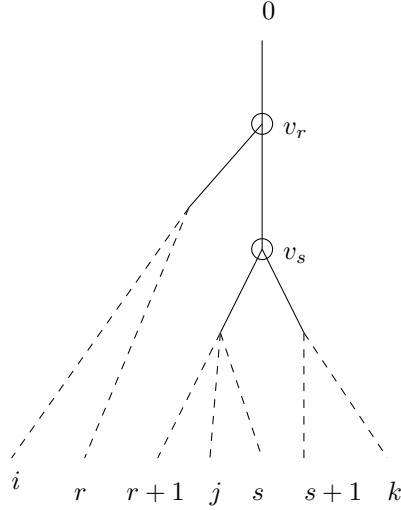


FIGURE 11. Comparing a cross-ratio with a simple ratio.

so that $z_0 = \infty$ we can write

$$\begin{aligned}
 \rho_{ijk0} &= -\frac{z_j - z_k}{z_j - z_i} \\
 &= -\frac{X_j + X_{j+1} + \dots + X_s + \dots + X_{k-1}}{X_i + X_{i+1} + \dots + X_r + \dots + X_{j-1}} \\
 &= -\frac{X_s}{X_r} \left(\frac{X_j/X_s + X_{j+1}/X_s + \dots + 1 + \dots + X_{k-1}/X_s}{X_i/X_r + \dots + 1 + \dots + X_{j-1}/X_r} \right).
 \end{aligned}$$

The ratios appearing in the big bracket are in general products of chart ratios corresponding to edges below v_r and v_s . The bracketed rational function is smooth for all positive non-zero ratios and continuous as ratios in the chart go to 0. Moreover $\rho_{ijk0} = 0$ if and only if $X_s/X_r = 0$.

Thus the cross-ratio charts define the same topology on \overline{M}_d as the simple ratio charts.

1.3. METRIC RIBBON TREES

In this section we introduce the space of metric ribbon trees. We have attempted to remain as consistent as possible with the notation of Fukaya and Oh in [4], and Nadler and Zaslow in [10].

Definition 1.3.1. A *based metric ribbon tree* is a quadruple (T, i, e_0, λ) of the following data:

- (a) T is a finite tree, with $d + 1$ semi-infinite exterior edges labeled e_0, \dots, e_d , and no vertex of valency 1 or 2. We denote by $E_{int}(T)$ the set of interior edges of T , which are all of finite length, and denote by $V_{int}(T)$ the set of interior vertices of T .
- (b) $i : T \hookrightarrow D \subset \mathbb{R}^2$ is an embedding of T in the closed unit disk such that the limit of the image of each the semi-infinite exterior edge e_i is a point in ∂D .
- (c) e_0 is a distinguished exterior edge of T , the *root*. The other exterior edges, e_1, \dots, e_d are called the *leaves*. The labeling e_0, e_1, \dots, e_d is consistent with their counterclockwise order on ∂D that comes from the embedding i .
- (d) $\lambda : E_{int}(T) \rightarrow \mathbb{R}_+$ is an *edge length map*, that assigns a non-negative real number to each interior edge.

Two based metric ribbon trees are *equivalent* if there is an isotopy of the closed disk which identifies all the data.

We use the same notation as in [4]: for a fixed integer $d > 2$ and a fixed root e_0 , we denote by Gr_d the set of all (T, i, e_0, λ) where T runs over all trees with $d + 1$ exterior edges and no vertices of valency 1 or 2. Denoting by $Gr(T)$ the set of all maps $\lambda : E_{int}(T) \rightarrow \mathbb{R}_+$, we can write

$$Gr_d = \bigcup_T Gr(T).$$

We now define a topology on $Gr(T)$. Assume that $\{\lambda_n\}_{n \in \mathbb{N}}$ is a sequence in $Gr(T)$, such that for each $e \in E_{int}(T)$ the sequence $\lambda_n(e)$ converges to $\lambda_\infty(e) \in [0, \infty)$. We define the limit of this sequence to be the quadruple (T', i', e'_0, λ') where

- (a) T' is the tree obtained from T by collapsing all edges with $\lambda_\infty(e) = 0$, and keeping all others. So T' is the image of a surjective morphism of planar rooted trees, $p : T \rightarrow T'$.
- (b) i' is the embedding obtained from the embedding i by contracting the collapsed edges.
- (c) e_0 is the end-vertex in T' corresponding to the end vertex in T .
- (d) For each edge $e \in E_{int}(T')$, we have that $p^{-1}(e) \in E_{int}(T)$, so we define $\lambda'(e) = \lambda_\infty(p^{-1}(e))$.

There is a natural partial order on the set of rooted planar trees with $d+1$ end vertices: namely, $T' \leq T$ if there exists a surjective morphism $p : T \rightarrow T'$ of rooted planar trees, or equivalently, T' is obtained from T by contracting a subset of its interior edges. Therefore, in the topology we have defined on $Gr(T)$, we can write its closure as

$$\text{cl } Gr(T) = \bigcup_{T' \leq T} Gr(T').$$

With respect to this topology, Gr_d is Hausdorff and closed.

The following is a theorem of Stasheff (see [13], [12]), proved also by Fukaya and Oh [4]. We give an elementary proof.

Theorem 1.3.2. *Gr_d is homeomorphic to \mathbb{R}^{d-2} .*

Proof. We show this by constructing a homeomorphism $\Theta : Gr_d \rightarrow M_d$, and the rest follows from the fact that M_d is homeomorphic to \mathbb{R}^{d-2} .

For each combinatorial type T we define $\Theta_T : Gr(T) \rightarrow M_d$ by

$$\begin{aligned} \lambda \in Gr(T) &\mapsto (X_1 : \dots : X_{d-1}) \in \mathbb{R}P^{d-2} \text{ where} \\ X_i &= \prod_{e \in [e_i, e_0] \cap [e_{i+1}, e_0]} e^{-\lambda(e)}. \end{aligned}$$

Here $[e_i, e_0]$ is shorthand for the unique non-self-crossing path in T from the leaf e_i back to the root. (For an exterior edge e , we take $\lambda(e) = 0$.)

The map Θ_T is a well-defined, continuous function of λ . It is injective since there is always a pair e_i, e_{i+1} such that their paths back to e_0 only intersect at e_0 , so $z_{i+1} - z_i = 1$ throughout the image of $Gr(T)$. This means that on the image of Θ_T , $X_i = 1$. So if $[\Theta_T(\lambda)] = [\Theta_T(\lambda')]$, we must have $z_i(\lambda) = z_i(\lambda')$ for all i . But then one can show inductively on the lengths of paths from the root e_0 , that $\lambda(e) = \lambda'(e)$ for all edges e in such a path, hence $\lambda = \lambda'$.

We also note that

$$\Theta_{T_1}(Gr(T_1)) \cap \Theta_{T_2}(Gr(T_2)) = \bigcup_{T < T_1, T_2} \Theta_T(Gr(T)).$$

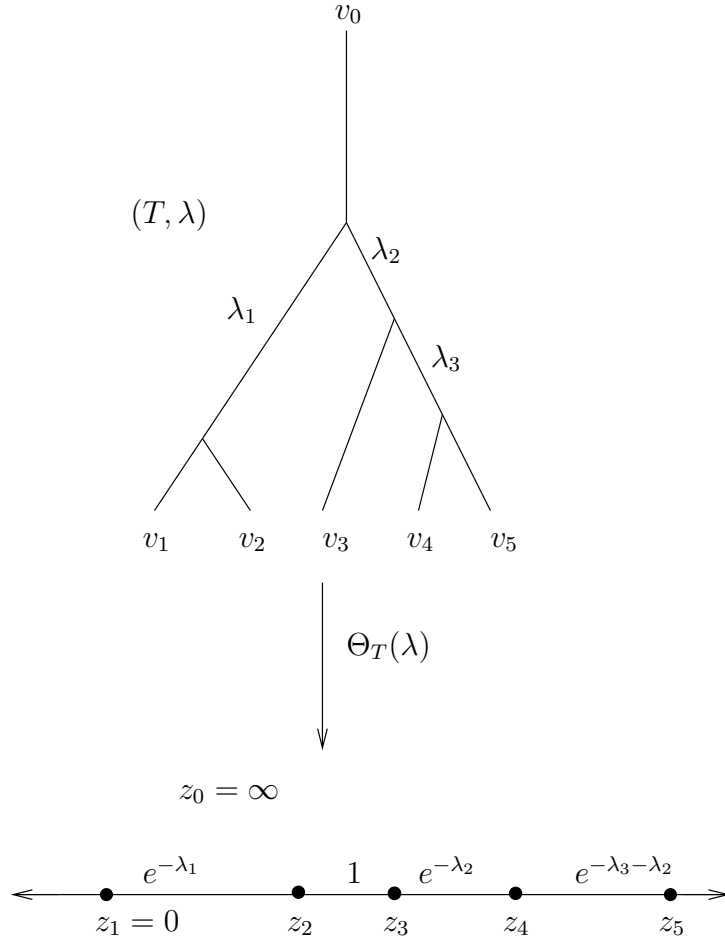


FIGURE 12. Identifying a metric ribbon tree in Gr_5 with a marked disk in M_5 .

To see that $\Theta : Gr_d \rightarrow M_d$ is surjective, we show that given any collection of d distinct points $z_1 < z_2 < \dots < z_d$, if we fix the parametrization so that $z_1 = 0$ and $\max(z_{i+1} - z_i) = 1$, this set of points, which we'll denote by Z , is in the image of some $\Theta_T(Gr(T))$. To reconstruct the combinatorial type T , we start by partitioning the set z_1, \dots, z_d into disjoint subsets of consecutive points, I_1, \dots, I_k say, by placing a partition between z_{i+1} and z_i if $z_{i+1} - z_i = 1$. Now form a tree with root e_0 , and k leaves $\tilde{e}_1, \dots, \tilde{e}_k$ indexed by the subsets I_1, \dots, I_k . For every subset I_j with at least 2 distinct points in it, we fix a dilation factor of e^{λ_j} so that $\max(z_{i+1} - z_i) = 1$ for $i \in I_j$. This in turn determines a partition of the set I_j , which determines leaves beneath \tilde{e}_j , and we set $\lambda(\tilde{e}_j) = \lambda_j$. Proceeding inductively in this way, one reconstructs the tree T and the edge lengths $\lambda \in Gr(T)$ such that $\Theta_T(\lambda) = Z$.

□

Remark 1.3.3. The map Θ can be thought of as an identification of each cone $Gr(T)$ with a homeomorphic cone in \mathbb{R}^{d-2} , in such a way that the identifications of the cones along their boundaries in \mathbb{R}^{d-2} are the same as the identifications along their boundaries in Gr_d , and the union of all the cones in \mathbb{R}^{d-2} is all of \mathbb{R}^{d-2} . To see this explicitly, fix the parametrization of configurations in M_d so that, for example, $z_d - z_{d-1} = 1$ and M_d is spanned by the coordinates X_1, \dots, X_{d-2} where $X_i = z_{i+1} - z_i$ and all X_i 's are positive. The images of the cones $Gr(T)$ are also cones in $\mathbb{R}_{>0}^{d-2}$, where the cones are centered at $(1, 1, \dots, 1)$ and their union is $\mathbb{R}_{>0}^{d-2}$. The map $(x, y) \mapsto (\log x, \log y)$ identifies $\mathbb{R}_{>0}^{d-2}$ with \mathbb{R}^{d-2} , and maps cones to cones.

Example 1.3.4. Consider the map $\Theta : Gr_4 \rightarrow M_4$. If we fix the parametrization of M_4 so that $z_2 - z_1 = 1$, the map Θ is a subdivision of $\mathbb{R}_{>0}^2$ into five cells, see Figure 13.

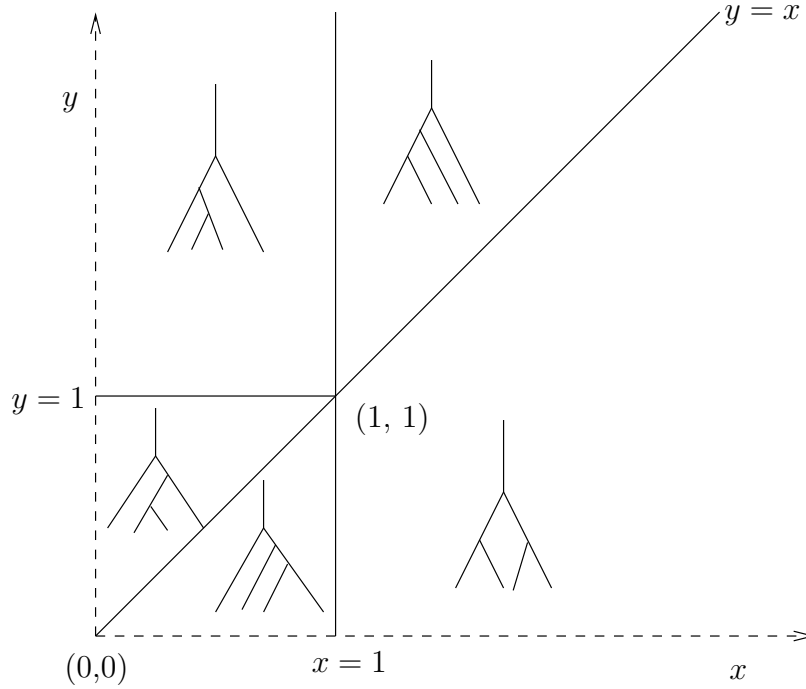


FIGURE 13. The images of the cones of Gr_4 in $\mathbb{R}_{>0}^2$. The map $(x, y) \mapsto (\log x, \log y)$ identifies them with cones in \mathbb{R}^2 whose union is all of \mathbb{R}^2 .

Each cell $Gr(T)$ is compactified by allowing the edge lengths to be infinite. We denote the induced compactification of Gr_d by \overline{Gr}_d . The map $\Theta : Gr_d \rightarrow M_d$ extends to a map $\Theta : \overline{Gr}_d \rightarrow \overline{M}_d$ by taking limits in appropriate charts.

Theorem 1.3.5. $\Theta : \overline{Gr}_d \rightarrow \overline{M}_d$ is a homeomorphism.

Proof. It follows from the observation that if λ is the edge-length in $Gr(T)$ assigned to an edge e , then in the chart $M(T) \subset \overline{M}_d$ the ratio X_i/X_j representing that same edge e has value $e^{-\lambda}$. Thus the image of a compactified cell $Gr(T)$ under the map Θ corresponds to the part of the chart $M(T)$ for which the ratios in the chart take values in $[0, 1]$. The boundary of \overline{Gr}_d , in which some edge lengths are infinite, maps to the boundary of \overline{M}_d , in which the corresponding ratios are zero. □

1.4. TORIC VARIETIES AND MOMENT POLYTOPES.

We now show that \overline{M}_d can be identified with the non-negative part of an embedded toric variety in $\mathbb{C}P^{k-1}$, where $k(d) = C_{d-1}$ is the $(d-1)$ -st Catalan number, which counts the number of binary planar rooted trees with d leaves. Each such tree determines a monomial in the $d-1$ variables X_1, X_2, \dots, X_{d-1} . The weight vector of the monomial is read directly from the combinatorics of the tree, according to the algorithm given by Loday in [8]. An immediate consequence of the theory of toric varieties (see for example [11], [5]) is that \overline{M}_d is homeomorphic to the moment polytope of the toric variety, which is the convex hull of the weight vectors.

Recall that a point in M_d can be identified with a configuration of d distinct, ordered points on \mathbb{R} , call them $z_1 < z_2 < \dots < z_d$, modulo translations and scaling. We get translational invariance by considering the variables

$$X_1 = z_2 - z_1, X_2 = z_3 - z_2, \dots, X_i = z_{i+1} - z_i, \dots, X_{d-1} = z_d - z_{d-1},$$

and the X_i 's are unique up to scalar multiplication, so are really projective coordinates,

$$\mathbf{X} = (X_1 : X_2 : \dots : X_{d-1}).$$

To every binary, planar, rooted tree T , we will now associate a weight vector $\mathbf{N}_T \in \mathbb{Z}^{d-1}$, using Loday's recipe. Each pair of adjacent leaves in T , labelled i and $i+1$ say, determines a unique vertex, which we call v_i , in T . Let a_i be the number of leaves on the left side of v_i , and let b_i be the number of leaves on the right side of v_i . Then the weight vector is

$$\mathbf{N}_T = (a_1 b_1, \dots, a_i b_i, \dots, a_{d-1} b_{d-1}).$$

The corresponding monomial is

$$\mathbf{X}^{\mathbf{N}_T} := \prod_{i=1}^{d-1} X_i^{a_i b_i}.$$

Example 1.4.1. For the tree pictured in Figure 14, the weight vector is $(1, 8, 3, 1, 2)$, so the corresponding monomial is $X_1 X_2^8 X_3^3 X_4 X_5^2$.

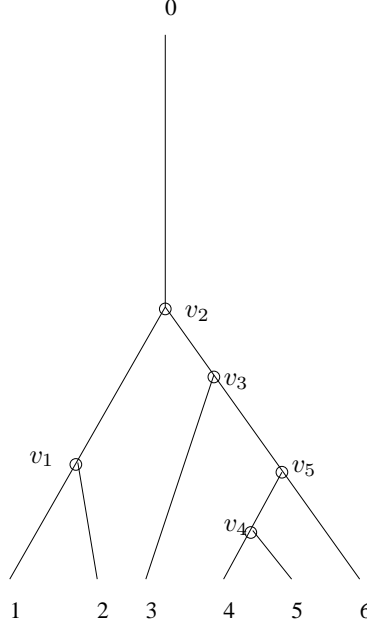


FIGURE 14. A binary, rooted, labelled tree. The labels on the leaves induce a labelling on the vertices.

Label the planar, binary rooted trees T_1, \dots, T_k . We define a projective toric variety $V \subset \mathbb{C}P^{k-1}$ by

$$(X_1 : \dots : X_{d-1}) \mapsto (\mathbf{X}^{N_{T_1}} : \dots : \mathbf{X}^{N_{T_k}})$$

The entries in the weight vectors always sum to $d(d-1)/2$, so the monomials all have the same degree and the map is well-defined on the homogeneous coordinates.

Definition 1.4.2. We say that two binary trees T and T' differ by a *flop* if there is an interior edge e of T and an interior edge e' of T' such that if e is contracted in T , and e' is contracted in T' , the resulting tree is the same (see Figure 15, in which the edges to be contracted are in bold).

Lemma 1.4.3. *Suppose that two maximal trees T and T' differ by a single flop across an edge e of T . Let R denote the simple ratio labeling the edge e in the chart determined by T . Then*

$$\frac{\mathbf{X}^{N_{T'}}}{\mathbf{X}^{N_T}} = R^m$$

for some integer $m > 0$. In general, for two trees T and T' ,

$$\frac{\mathbf{X}^{N_{T'}}}{\mathbf{X}^{N_T}} = R_{i_1}^{m_1} R_{i_2}^{m_2} \dots R_{i_r}^{m_r}$$

for some ratios R_{i_1}, \dots, R_{i_r} in the ratio chart associated to T and positive integers m_1, \dots, m_r .

Proof. First let us consider the case of a single flop. Without loss of generality consider the situation in Figure 15. Say T is on the left, and T' is on the right, and the affected edges are in bold. The weight vectors \mathbf{N}_T and $\mathbf{N}_{T'}$ are the same in all entries except

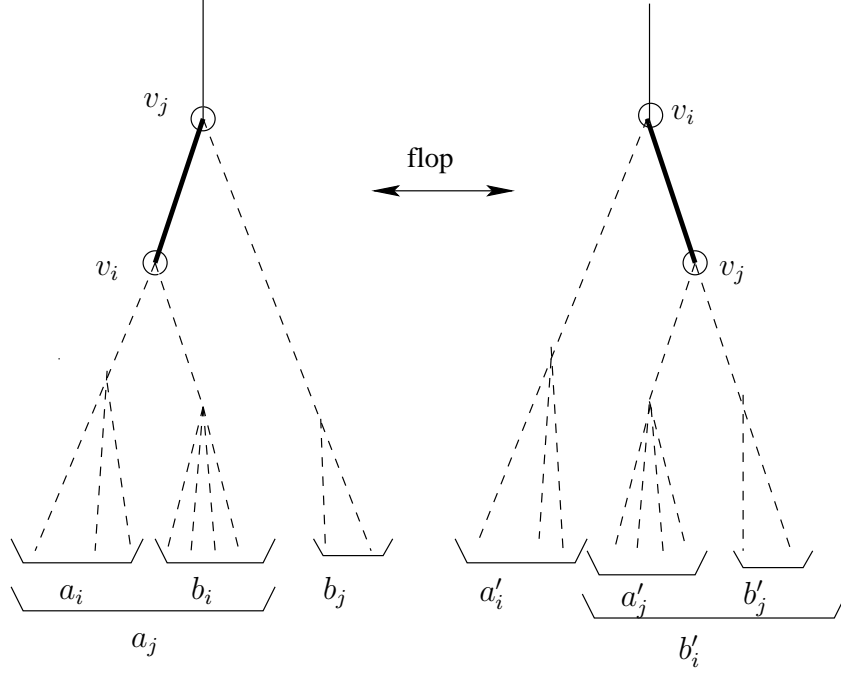


FIGURE 15. Two trees differ by a single flop if a single interior edge can be contracted in each of them to produce the same tree.

entries i and j , where

$$\begin{aligned} (\mathbf{N}_T)_i &= a_i b_i, \\ (\mathbf{N}_T)_j &= a_j b_j = (a_i + b_i) b_j \\ (\mathbf{N}_{T'})_i &= a_i (b_i + b_j), \\ (\mathbf{N}_{T'})_j &= b_i b_j. \end{aligned}$$

Therefore,

$$\begin{aligned} \frac{\mathbf{X}^{\mathbf{N}_{T'}}}{\mathbf{X}^{\mathbf{N}_T}} &= \frac{X_i^{a_i(b_i+b_j)} X_j^{b_i b_j}}{X_i^{a_i b_i} X_j^{(a_i+b_i) b_j}} \\ &= \frac{X_i^{a_i b_j}}{X_j^{a_i b_j}} \\ &= \left(\frac{X_i}{X_j} \right)^{a_i b_j} \end{aligned}$$

and observe that X_i/X_j is the ratio labeling that edge of T .

The vertices are partially ordered by their positions in the tree; the effect of a flop on the partial ordering is a single change, $(v_i \leq v_j) \mapsto (v_j \leq v_i)$, in between a pair of vertices which are adjacent in the partial order. In general, every maximal tree is obtained from a *fixed* tree T by a sequence of independent flops – by independent we just mean that each flop involves a different pair of vertices.

So to prove the general case we can do induction on the number of independent flops needed to get from a fixed maximal tree T , to any other maximal tree T' . We have already proved the base case, so consider a tree T' obtained after a sequence of $k + 1$ flops. Write \tilde{T} for a tree which is k independent flops away from T and one flop away from T' . Suppose that the the final flop between \tilde{T} and T' is described by the change $(v_i \leq v_j) \mapsto (v_j \leq v_i)$ for a pair of adjacent vertices v_i and v_j . By the inductive hypothesis and the base step,

$$\begin{aligned} \frac{\mathbf{X}^{\mathbf{N}_{T'}}}{\mathbf{X}^{\mathbf{N}_T}} &= \frac{\mathbf{X}^{\mathbf{N}_{T'}} \mathbf{X}^{\mathbf{N}_{\tilde{T}}}}{\mathbf{X}^{\mathbf{N}_{\tilde{T}}} \mathbf{X}^{\mathbf{N}_T}} \\ &= \left(\frac{X_i}{X_j} \right)^m R_{i_1}^{m_1} R_{i_2}^{m_2} \dots R_{i_r}^{m_r} \end{aligned}$$

for some positive integers m_1, \dots, m_r and m , and some ratios R_{i_1}, \dots, R_{i_r} in the chart for T . Since none of the previous flops involved the pair v_i and v_j , the partial order in the original tree T must have also had $v_i \leq v_j$, although they were possibly not adjacent in T . In any case, the ratio X_i/X_j is a product of ratios for the edges in the path from v_i to v_j . This completes the inductive step. \square

Theorem 1.4.4. \overline{M}_d is homeomorphic to the non-negative part of the projective toric variety V .

Proof. We show that each chart $M(T_i)$ is identified with the non-negative part of the affine slice $V \cap \mathbb{A}_i$, where

$$\mathbb{A}_i = (\xi_1 : \xi_2 : \dots : \underbrace{1}_{i^{th}} : \dots : \xi_k).$$

We prove it for the the first affine piece. $V \cap \mathbb{A}_1$ consists of all points

$$\left(1 : \frac{\mathbf{X}^{\mathbf{N}_{T_2}}}{\mathbf{X}^{\mathbf{N}_{T_1}}} : \dots : \frac{\mathbf{X}^{\mathbf{N}_{T_k}}}{\mathbf{X}^{\mathbf{N}_{T_1}}} \right)$$

where the ratios are allowed to be 0. Lemma 1.4.3 says that for any edge in T_1 , with ratio say X_i/X_j , there is an entry $(X_i/X_j)^m$ in the slot belonging to the tree obtained by a flop of that edge. Note that for any positive integer m , the map $r \mapsto r^m$ is a homeomorphism for $r \in [0, \infty)$, which is the domain of the ratios in the chart $M(T_1)$. The other entries are higher products of ratios in $M(T_1)$ so depend smoothly on the chart $M(T_1)$. Therefore $M(T_1)$ is homeomorphic to the non-negative part of $V \cap \mathbb{A}_1$.

□

Corollary 1.4.5. \overline{M}_d is homeomorphic to a polytope in \mathbb{R}^{d-1} which is the convex hull of the weight vectors. It is also homeomorphic to the Stasheff associahedron K_d .

Proof. The non-negative part of a projective toric variety constructed with weight vectors is homeomorphic, via the moment map, to the convex hull of the weight vectors (see, for example, [5], [11]). The proof that it is also homeomorphic to the Stasheff associahedron K_d is by induction on d : the one-dimensional spaces \overline{M}_3 and K_3 are both compact and connected, and so homeomorphic. It suffices, therefore, to show that $\overline{M}_{d,1}$ is the cone on its boundary – and this is automatically true since it is homeomorphic to a polytope. □

Part 2. The multiplihedron, quilted disks, and bicolored metric trees.

2.1. THE MULTIPLIHEDRON.

Stasheff also introduced a family of *CW*-complexes called the *multiplihedra*, which play the same role for loop or A_∞ spaces as the associahedra play in the recognition principle for loop spaces. The d -th multiplihedron J_d is a complex of dimension $d - 1$ whose vertices correspond to ways of bracketing d variables x_1, \dots, x_d and applying an operation, say f . The multiplihedron J_3 is the hexagon shown in Figure 16.

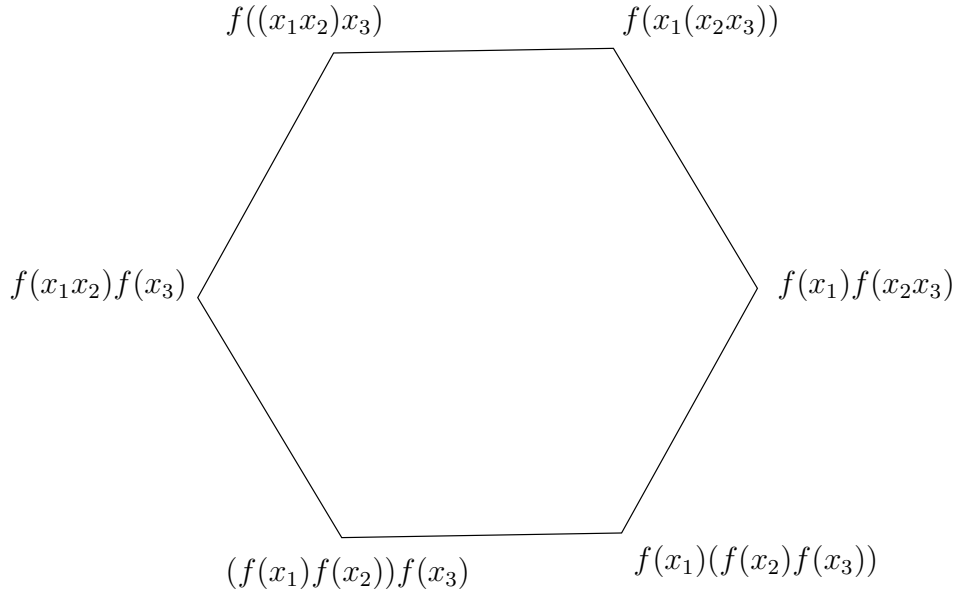


FIGURE 16. Vertices of J_3

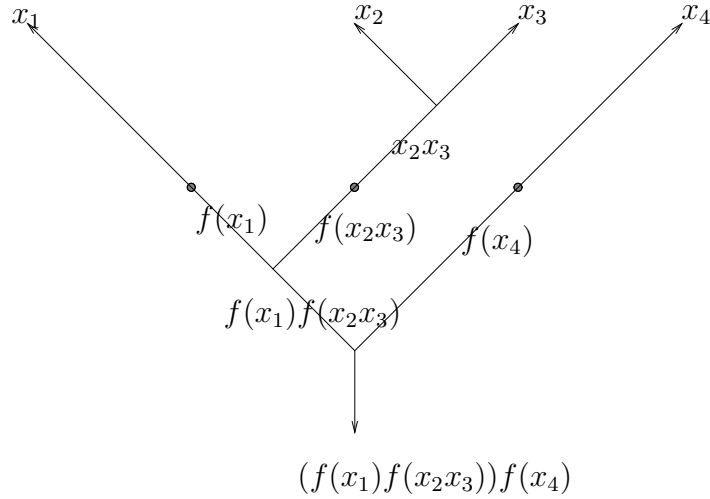


FIGURE 17. Tree for $(f(x_1)f(x_2x_3))f(x_4)$

The facets of J_d are of two types. First, there are the images of the inclusions

$$J_{i_1} \times \dots \times J_{i_j} \times K_j \rightarrow J_d$$

for partitions $i_1 + \dots + i_j = d$, and secondly the images of the inclusions

$$J_{d-e+1} \times K_e \rightarrow J_d$$

for $2 \leq e \leq d$. One constructs the multiplihedron inductively starting from setting J_2 and K_3 equal to closed intervals.

Each vertex corresponds to a rooted tree with two types of vertices, the first a trivalent vertex corresponding to a bracketing of two variables and the second a bivalent vertex corresponding to an application of f .

Dualizing the rooted tree gives a triangulation of the $d+1$ -gon together with a partition of the two-cells into two types, depending on whether they occur before or after a bivalent vertex in a path from the root.

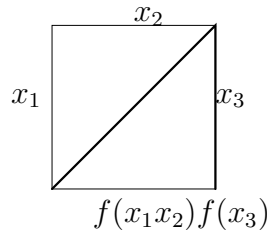


FIGURE 18. Triangulation corresponding to $f(x_1x_2)f(x_3)$

The edges of J_d are of two types:

(a) A change in bracketing

$$\dots x_{i-1}(x_i x_{i+1}) \dots \mapsto (x_{i-1} x_i) x_{i+1}$$

(a flop of the type shown in Figure 7) or vice-versa

(b) A move of the form

$$\dots f(x_i x_{i+1}) \dots \mapsto f(x_i) f(x_{i+1}) \dots$$

or vice versa, which corresponds to moving one of the bivalent vertices past a trivalent vertex, after which it becomes a pair of bivalent vertices, or vice-versa:

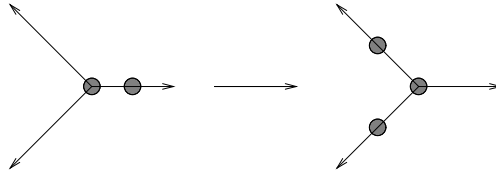


FIGURE 19. Splitting of bivalent vertices

2.2. MODULI SPACES OF QUILTED DISKS

In this section, a *quilted disk* refers to the unit disk $D \subset \mathbb{C}$ together with a circle $C \subset D$ (the *seam* of the quilt) tangent to a unique point in the boundary. Thus C divides the interior of D into two components. Given quilted disks (D_0, C_0) and (D_1, C_1) , a morphism from (D_0, C_0) to (D_1, C_1) is a holomorphic isomorphism $D_0 \rightarrow D_1$ mapping C_0 to C_1 . Any quilted disk is isomorphic to the pair (D, C) where D is the unit disk in the complex plane and C the circle of radius $1/2$ passing through 1 and 0 . Consider the map $D \rightarrow H$ given by $z \mapsto -i/(z-1)$. The image of C is the horizontal line L through i . Thus the automorphism group of (H, L) is the group $T \subset SL(2, \mathbb{R})$ of translations by real numbers.

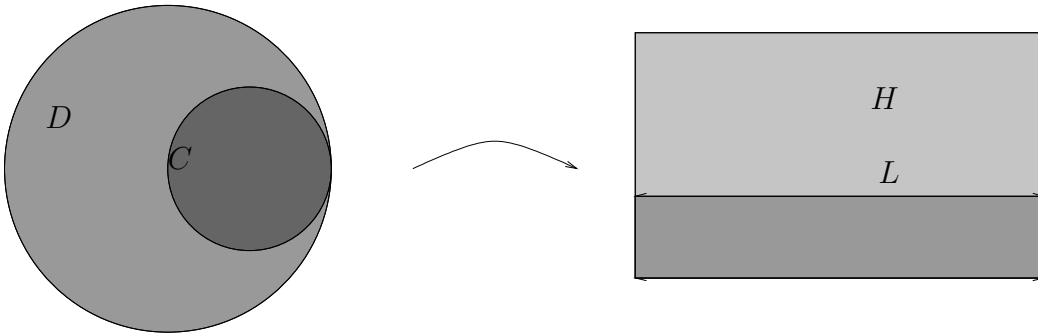


FIGURE 20. Quilted disk as a quilted half-plane

Let $d \geq 2$. A quilted disk with $d + 1$ markings on the boundary consists of the unit disk $D \subset \mathbb{C}$, distinct points $z_0, \dots, z_d \in \partial D$ and a circle $C \subset D$ tangent to z_0 , of radius between 0 and 1. A morphism $(D_0, C_0; z_0, \dots, z_d) \rightarrow (D_1, C_1; w_0, \dots, w_d)$ is a holomorphic isomorphism $D_0 \rightarrow D_1$ mapping C_0 to C_1 and z_j to w_j for $j = 0, \dots, d$. Let $M_{d,1}$ be the set of isomorphism classes of $d + 1$ -marked quilted disks. We compactify $M_{d,1}$ as follows. A *nodal* $(d + 1)$ -*quilted disk* S is a collection of quilted and unquilted marked disks, identified at pairs of points on the boundary. The combinatorial type of S is a graph Γ with two types of vertices, depending on whether the corresponding disk component is quilted or not. We require that

- (a) The combinatorial type of S is a tree.
- (b) Each unquilted disk component contains at least 3 singular or marked points.
- (c) Each quilted disk component is attached to only unquilted components;
- (d) The unique non-self-crossing path from the semi-infinite edge marked z_0 to the semi-infinite edge z_j crosses exactly one quilted vertex, for each $j = 1, \dots, d$.

A nodal quilted disk is called *semistable* if

- (a) Each quilted disk component contains at least 2 singular or marked points;
- (b) Each unquilted disk component contains at least 3 singular or marked points.

Thus the automorphism group of any disk component is trivial, and from this one may derive that the automorphism group of any semistable $d + 1$ -marked nodal quilted disk is also trivial.

Remark 2.2.1. The appearance of the two kinds of disks can be explained by the following bubbling considerations. Suppose that D_α is a sequence in $M_{d,1}$. For any sequence of rescalings $\varphi_\alpha : D_\alpha \rightarrow D_\alpha$ consider the following set of real numbers:

$$\text{dist}(z_{\alpha,i}, z_{\alpha,j}), \text{dist}(z_{\alpha,i}, C_\alpha), \text{dist}(C_\alpha, \partial D_\alpha).$$

We say that a subset of $\{z_{\alpha,i}, C_\alpha\}$ of size at least 3 is *on the same scale* if after some sequence of re-scalings, the distances approach finite, non-zero values. An *admissible sequence of rescalings* is one for which some subset of size at least 3 is on the same scale. Two admissible sequences of rescalings are *equivalent* if the numbers above have the same limits. Each admissible sequence of rescalings defines a partition of the $\{z_{\alpha,i}\}$ according to which points have zero distance limit after the rescaling. That is, we say

$$z_{\alpha,i} \sim_{\varphi_\alpha} z_{\alpha,j}$$

if

$$\text{dist}(\varphi_\alpha(z_{\alpha,i}), \varphi_\alpha(z_{\alpha,j})) \rightarrow 0, \quad \alpha \rightarrow \infty.$$

Each admissible sequence of rescalings gives rise to a bubble in the limit, of three kinds: Either $C_\alpha \rightarrow \partial D_\alpha$ in the limit, in which case we say that the resulting bubble has no interior circle (the circle is now at radius 1), or C_α approaches a circle of radius in $(0, 1)$, in which case we say that the bubble *has interior circle*, or the radius approaches zero,

in which case we say that the bubble *has no interior circle*. Thus the limiting sequence is a bubble tree, whose bubbles are of the two types discussed above.

Let $\overline{M}_{d,1}$ denote the set of isomorphism classes of semistable $d+1$ -marked nodal quilted disks.

Example 2.2.2. $\overline{M}_{3,1}$ is a hexagon, see Figure 21.

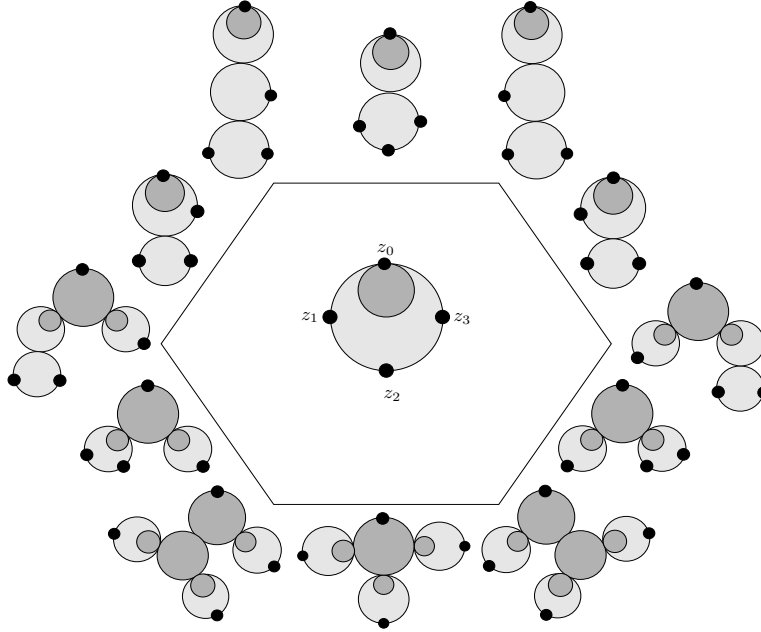


FIGURE 21. $\overline{M}_{3,1}$

2.2.1. Topology via cross-ratios. We introduce a topology on $\overline{M}_{d,1}$ via cross-ratios, as in the previous section for the moduli space of semistable nodal marked disks. Let D denote the unit disk, C a circle in D passing through a unique point z_0 and $z_1, z_2 \in D$ points in D such that z_0, z_1, z_2 are distinct. Let w be a point in C not equal to z_0 . Define

$$\rho_{3,1}(D, C, z_1, z_2) = \text{Im}(\rho(z_0, z_1, z_2, w)).$$

$\rho_{3,1}$ is independent of the choice of w and invariant under the group of automorphisms of the disk and so defines a map

$$\rho_{3,1} : M_{3,1} \rightarrow (0, \infty).$$

We extend $\rho_{3,1}$ to $\overline{M}_{3,1}$ by setting $\rho_{3,1}(S) = 0$ if S is the 3-marked quilted nodal disk with three components, and $\rho_{3,1}(S) = \infty$ if S is the 3-marked nodal disk with two components. Thus $\rho_{3,1}$ extends to a bijection

$$\rho_{3,1} : \overline{M}_{3,1} \rightarrow [0, \infty].$$

More generally, given $d \geq 3$ and a pair i, j of distinct, non-zero vertices, let Γ_{ij} denote the minimal connected subtree of Γ containing the seminfinite edges corresponding to z_i, z_j, z_0 . There are three possibilities for Γ_{ij} , depending on whether the quilted vertex appears closer or further away than the trivalent vertex from z_0 , or equals the trivalent vertex.

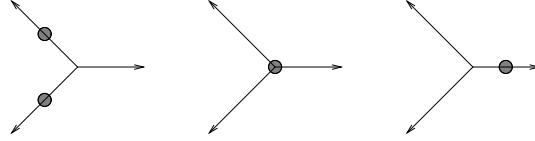


FIGURE 22. Tree types for J_3

If the first, resp. third case define $\rho_{ij}(S) = 0$ resp ∞ . In the second case let (D, C) denote the disk component corresponding to the trivalent vertex, $w_i, w_j \in \partial D$ the points corresponding to the semiinfinite edges labelled z_i, z_j , and define

$$\rho_{ij}(S) = \rho_{3,1}(D, C, w_i, w_j).$$

In addition, for any four distinct indices i, j, k, l we have the cross-ratio

$$\rho_{ijkl} : \overline{M}_{d,1} \rightarrow [0, \infty]$$

defined in the previous section, obtained by treating the quilted disk component as an ordinary component. Consider the map

$$\rho_{d1} : \overline{M}_{d,1} \rightarrow \mathbb{R}^{(d+1)d(d-1)(d-2)/4! + d(d-1)/2}$$

obtained from all the cross-ratios. Given an element $S \in \overline{M}_{d,1}$, the combinatorial type of S can be obtained from examining which cross-ratios are 0 or ∞ . First, ignoring types of vertices the tree Γ can be obtained from the cross-ratios ρ_{ijkl} . The cross-ratios ρ_{ij} determine whether the trivalent vertex of the tree Γ_{ij} is on the same side of the quilted vertices as z_0 or not. In addition, the isomorphism class of each disk component of S is determined by the cross-ratios ρ_{ijkl} and ρ_{ij} with values in $(0, \infty)$. Thus the map $\rho_{d,1}$ is injective and we define the topology on $\overline{M}_{d,1}$ by pulling back the topology on the codomain. Since the codomain is Hausdorff and compact, so is $\overline{M}_{d,1}$.

Remark 2.2.3. As before, the maps $\overline{M}_{d,1} \rightarrow \overline{M}_4$, $\overline{M}_{d,1} \rightarrow \overline{M}_{3,1}$ are special cases of forgetful morphisms constructed as follows. For any subset $I \subset \{0, \dots, n\}$ of size k we have a forgetful morphism

$$\overline{M}_{d,1} \mapsto \overline{M}_k$$

obtained by forgetting the position of the circle and collapsing all unstable components. The map

$$\overline{M}_{d,1} \mapsto \overline{M}_d$$

deserves special mention. Its fiber over an element $S \in \overline{M}_d$ consists of a union of point and intervals whose number is the maximal length of a path from z_0 to $z_i, i \neq 0$ in the

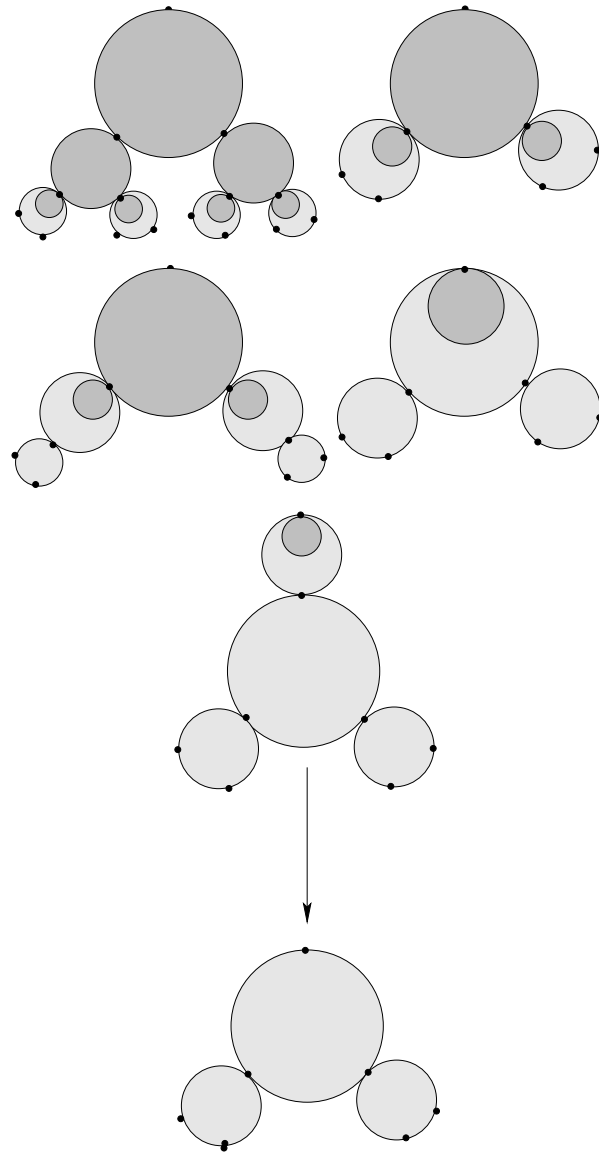


FIGURE 23. A fiber in $\overline{M}_{4,1} \rightarrow \overline{M}_4$. The projection forgets the inner circle and then collapses any unstable components to a point.

combinatorial type of S (resp. minus one). Shown in Figure 23 is a fiber consisting of three points and two open intervals.

Similarly, for any subset $J \subset \{1, \dots, n\}$ of size l we have a forgetful morphism

$$\overline{M}_{d,1} \mapsto \overline{M}_{l,1}$$

obtained by forgetting the positions of $z_j, j \notin J$ and collapsing all unstable disk components. By definition, the topology on $\overline{M}_{d,1}$ is the minimal topology such that all forgetful morphisms are continuous and the topology on $\overline{M}_{3,1} \cong [0, \infty]$, $\overline{M}_4 \cong [0, \infty]$ is induced by the cross-ratio.

2.2.2. Properties of the cross-ratio coordinates. The properties of the coordinates ρ_{ijkl} are listed in Section 1.2.2, and remain the same. For the coordinates $\rho_{i,j}$ there are similar properties, whose proofs (which we omit) are very minor modifications of the proofs for ρ_{ijkl} :

(Invariance): For all $p \in \overline{M}_d$, and for all $\phi \in SL(2, \mathbb{R})$, $\rho_{i,j}(\phi(p)) = \rho_{i,j}(p)$.

(Symmetry): $\rho_{i,j} = -\rho_{j,i}$.

(Normalization): $\rho_{i,j} = \begin{cases} \infty, & \text{if } i \neq j \text{ and } L = \infty, \\ 0, & \text{if } i \neq j \text{ and } L = \mathbb{R}. \end{cases}$

(Recursion):

$$(5) \quad \rho_{i,k} = \frac{\rho_{i,j}}{\rho_{j,k}}$$

Finally, the two types of coordinate are related by

(Relations):

$$(6) \quad \rho_{j,k} = \frac{\rho_{i,j}}{-\rho_{ijk0}}$$

$$(7) \quad \rho_{i,k} = \frac{\rho_{i,j}}{1 - \rho_{ijk0}}.$$

To prove (6), pick a component of the nodal disk on which z_i, z_j and z_0 are distinct. Picking some $\zeta \in C$, without loss of generality we may set $z_i = 0, z_j = 1, z_0 = \infty, z_k = \rho_{ij0k}$ and $\zeta = \rho_{ij0\zeta}$. Then we have,

$$\begin{aligned} \rho_{jk0\zeta} &= \frac{(z_k - z_0)(\zeta - z_j)}{(z_j - z_k)(z_0 - \zeta)} \\ &= \frac{-(\rho_{ij0\zeta} - 1)}{1 - \rho_{ij0k}} \\ &= \frac{(\rho_{ij0\zeta} - 1)}{\rho_{ij0k} - 1} \\ &= \frac{\rho_{ij0\zeta} - 1}{-\rho_{ijk0}} \end{aligned}$$

Equating imaginary parts yields (6). The proof of (7) is almost identical.

2.2.3. Charts using cross-ratios. As in the case of the moduli space of nodal disks, one can use the cross-ratios to define local charts on the space of quilted disks, $\overline{M}_{d,1}$.

However, $\overline{M}_{d,1}$ is *not* a manifold-with-corners. We say that a point $S \in \overline{M}_{d,1}$ is a *singularity* if $\overline{M}_{d,1}$ is not combinatorially a manifold with corners near S .

Example 2.2.4. The first singular point occurs for $d = 4$. The expression $(f(x_1)f(x_2))(f(x_3)f(x_4))$ is adjacent to the expressions

$$\begin{aligned} &f(x_1x_2)(f(x_3)f(x_4)), \quad (f(x_1)f(x_2))f(x_3x_4) \\ &f(x_1)(f(x_2)(f(x_3)f(x_4))), \quad ((f(x_1)f(x_2))f(x_3))f(x_4) \end{aligned}$$

and hence there are four edges coming out of the corresponding vertex. On the other hand, the dimension of $M_{4,1}$ is 3, see Figure 24. Thus $M_{4,1}$ cannot be a manifold with corners (and therefore, not a simplicial polytope.)

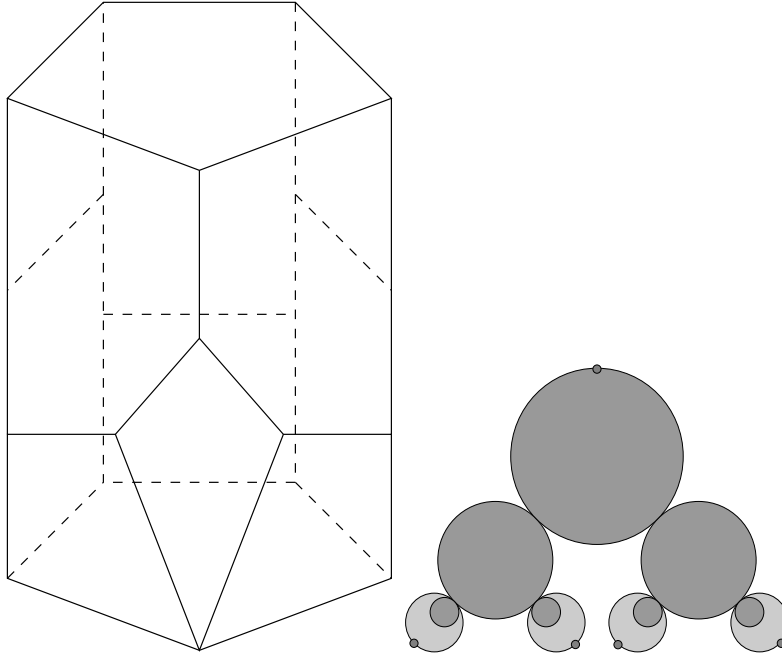


FIGURE 24. $\overline{M}_{4,1}$, sometimes called the “Chinese lantern”. The singular point on the boundary, which has 4 edges coming out of it, corresponds to the nodal quilted disk at right.

Let $\Gamma_{d,1}$ be a combinatorial type in $\overline{M}_{d,1}$. A cross-ratio chart associated to $\Gamma_{d,1}$ consists of

- (a) $n - 3$ cross-ratios for each disk component in $\Gamma_{d,1}$ that has n special features, where a special feature is either a marked point, a nodal point, or an inner circle of radius $0 < r < 1$;

- (b) a coordinate $\rho_{abcd} = 0$ for each finite edge in Γ that is incident at each end to a trivalent vertex;
- (c) a coordinate $\rho_{a,b} = 0$ for each finite edge in Γ that is incident to a *bivalent* colored vertex from above, and a coordinate $1/\rho_{a,b} = 0$ for each finite edge in Γ that is incident to a bivalent colored vertex from below,
- (d) $k - 1$ relations among these coordinates, where k is the number of colored vertices in Γ .

Rather than computing formulas for the $(k - 1)$ relations between the cross-ratios in our chart, we will return to them in the next section after introducing an equivalent collection of charts on $\overline{M}_{d,1}$, in which the relations are far simpler.

Proposition 2.2.5. *Let $p \in \overline{M}_{d,1}$. Suppose that p has combinatorial type $\Gamma_{d,1}$ with k colored vertices, and suppose that a set of chart coordinates has been chosen following (a), (b) and (c) above. Then, in a neighborhood of p , all cross-ratios $\rho_{i,j,k,l}$ and $\rho_{i,j}$ are smooth functions of those in the chart.*

Proof. First we prove that all cross-ratios of the form ρ_{ijkl} are smooth functions of those in the chart associated to $\Gamma_{d,1}$. Denote by Γ_d the combinatorial type in \overline{M}_d obtained from $\Gamma_{d,1}$ by forgetting colored vertices. Taking all cross-ratios of the form ρ_{ijkl} in the chart associated to $\Gamma_{d,1}$ almost gives a chart for Γ_d in the sense of Section 1.2.3. The only coordinates that might be missing for the chart are those corresponding to edges that have a bivalent colored vertex on them. For each bivalent vertex, we can assume that the lower edge has coordinate $\rho_{i,j} = \infty$ and the upper edge is either $\rho_{j,k} = 0$ or $\rho_{h,i} = 0$. Assuming the first case, relation (6) holds and

$$\rho_{i,j,k,0} = \frac{-\rho_{i,j}}{\rho_{j,k}},$$

expressing $\rho_{i,j,k,0}$ as a smooth function of the chart coordinates, and $\rho_{i,j,k,0}$ is a valid chart coordinate for the underlying edge in Γ_d . The other case is very similar, by relation (6),

$$\rho_{h,i,j,0} = \frac{-\rho_{h,i}}{\rho_{i,j}},$$

expresses $\rho_{h,i,j,0}$ as a smooth function of the chart coordinates, and $\rho_{h,i,j,0}$ is a valid chart coordinate for the underlying edge in Γ_d . Hence we get a valid chart for Γ_d . Now by Theorem 1.2.2 all cross-ratios of the form ρ_{abcd} are smooth functions of the chart coordinates.

Finally, relations (6) and (7) can be used to obtain all cross-ratios of the form $\rho_{a,b}$ from the cross-ratios of the form $\rho_{i,j}$ in the chart, and the appropriate ρ_{ijk0} 's. \square

2.2.4. Charts using simple ratios. Choosing parametrizations such that $z_0 = \infty$, the elements of $M_{n,1}$ can be identified with configurations of n distinct points $-\infty < z_1 < z_2 < \dots < z_n < \infty$ in $\mathbb{R} \subset \mathbb{C}$, together with a horizontal line L in the upper half plane

of \mathbb{C} , modulo transformations of the form $z \mapsto az + b$ for $a, b \in \mathbb{R}$ such that $a > 0$, i.e. dilation and translation. For such configurations define coordinates $(X_1, X_2, \dots, X_n, Y)$ by $X_i = z_{i+1} - z_i$, and $Y = \text{dist}(L, \mathbb{R})$. A transformation $z \mapsto az + b$ for $a, b \in \mathbb{R}$ sends

$$(X_1, X_2, \dots, X_{n-1}, Y) \mapsto (aX_1, aX_2, \dots, aX_{n-1}, aY),$$

so they are really projective coordinates, $(X_1 : X_2 : \dots : X_{n-1} : Y)$.

We construct new charts as follows. Each maximal bicolored tree has two types of edges: those that connect a pair of vertices v_i and v_j in the underlying graph, and those that connect a vertex v_i with either a colored vertex below it, or a colored vertex above it. For an edge of the first type: if the vertex v_i is below the vertex v_j , then the associated ratio is X_i/X_j . For an edge of the second type: if the vertex v_i is immediately below the colored vertex, then the associated ratio is Y/X_i ; if the vertex v_i is immediately above the colored vertex, the associated ratio is X_i/Y . Denote the subset of $M_{d,1}$ that is covered by a ratio chart corresponding to a maximal bicolored tree T by $M(T)$.

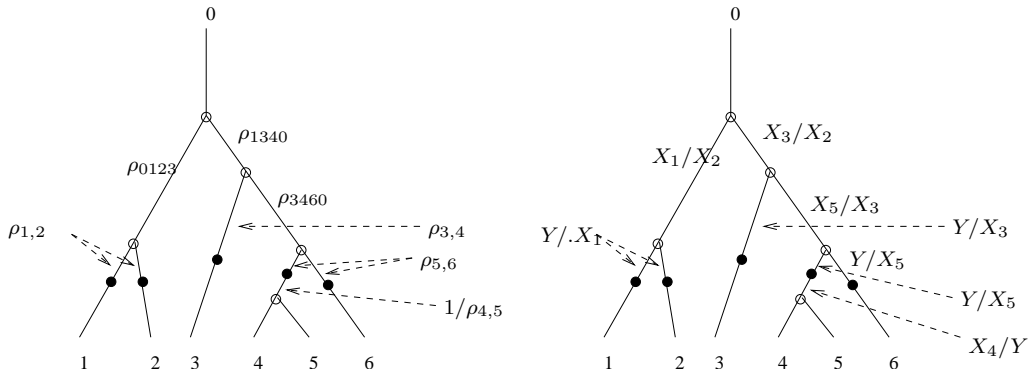
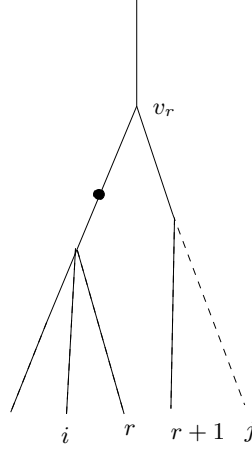


FIGURE 25. A cross-ratio chart and a simple-ratio chart for the same maximal bicolored tree.

2.2.5. Equivalence of charts. We show that each cross-ratio in the chart is a smooth function of the simple ratios, and is zero if and only if the corresponding simple ratio is zero. To show the other direction – that the simple ratios are smooth functions of the cross-ratios – is an argument that is similarly straightforward so we will not include it. We note again that if vertex v_i is below vertex v_j in the tree, then the ratio X_i/X_j is a product of the ratios representing the edges joining the vertex v_i to v_j . Hence the proof for a cross-ratio ρ_{ijk0} or ρ_{0ijk} follows from the proof given already in the case of ordinary trees. The only case that isn't already covered is that of a cross-ratio $\rho_{i,j}$ in the chart. Parametrizing so that $z_0 = \infty$ and using Y to denote the height of the line with respect to this parametrization, consider an edge such as the one pictured in 26, where the cross-ratio assigned to it in the cross-ratio chart is $\rho_{i,j}$, while the simple ratio assigned to it is Y/X_r . Then we can write


 FIGURE 26. Comparing a cross-ratio $\rho_{i,j}$ with a ratio Y/X_r .

$$\begin{aligned}
 \rho_{i,j} &= \frac{Y}{z_j - z_i} \\
 &= \frac{Y}{X_i + \dots + X_r + \dots + X_{j-1}} \\
 &= \frac{Y}{X_r} \left(\frac{1}{\frac{X_i}{X_r} + \dots + 1 + \dots + \frac{X_{j-1}}{X_r}} \right)
 \end{aligned}$$

where the ratios appearing in the big bracket are products of chart ratios corresponding to edges below v_r . The bracketed rational function is smooth and invertible for all positive non-zero ratios and it is continuous as ratios in the chart go to 0. Moreover $\rho_{i,j} = 0$ if and only if $Y/X_r = 0$. The other case, of a colored vertex above a regular vertex, is very similar so we omit it.

So the charts of simple ratios define the same topology on $\overline{M}_{d,1}$ as the charts of cross-ratios.

2.3. BICOLORED METRIC RIBBON TREES.

Definition 2.3.1. A *bicolored metric ribbon tree* is a quintuple $(T, i, e_0, V_{col}, \lambda)$. T is a tree with semi-infinite exterior edges labeled e_0, e_1, \dots, e_d , with e_0 distinguished as the “root” of the tree, while e_1, \dots, e_d are called the “leaves”. The map $i : T \rightarrow D$ is an embedding of T into the unit disk such that the images of the exterior edges have a limit point on the boundary of D , with the limit points of e_0, \dots, e_d cyclically ordered following the counter clockwise orientation of ∂D . $V_{col} \subset V_{int}(T)$ is a collection of *colored vertices*, and $\lambda : E_{int}(T) \rightarrow \mathbb{R}_+$ is a map of edge lengths, subject to the following conditions.

- (a) In any non-self-crossing path from a leaf $e_i \in \{e_1, \dots, e_d\}$ back to the root, exactly one interior vertex in that path is a colored vertex.
- (b) If a vertex $v \in V(T)$ is bivalent, then $v \in V_{col}$.
- (c) The edge length map λ satisfies the condition that the sum of the edge lengths in any non-self-crossing path from a colored vertex $v \in V_{col}$ back to the root is independent of $v \in V_{col}$.

Example 2.3.2. For the tree in Figure 27, an edge length map is subject to the relations

$$\begin{aligned}
 \lambda_1 + \lambda_2 + \lambda_3 &= \lambda_1 + \lambda_2 + \lambda_4 \\
 &= \lambda_1 + \lambda_2 + \lambda_5 \\
 &= \lambda_1 + \lambda_6 \\
 &= \lambda_7.
 \end{aligned}$$

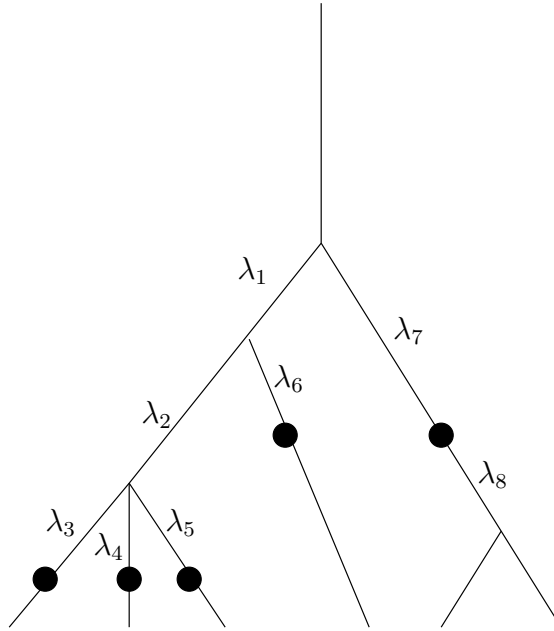


FIGURE 27. A bicolored ribbon tree. The relations on $\lambda_1, \dots, \lambda_8$ imply that $\lambda_3 = \lambda_4 = \lambda_5$, $\lambda_3 + \lambda_2 = \lambda_6$, and $\lambda_6 + \lambda_1 = \lambda_7$.

For each tuple (T, V_{col}) satisfying conditions a and b, we denote by $Gr(T, V_{col})$ the set of all maps λ satisfying condition c, and then write

$$G_{k,1} = \bigcup_{(T, V_{col})} Gr(T, V_{col}).$$

We define a topology on $Gr(T, V_{col})$ as follows. Assume that a sequence $\{\lambda_n\}_{n \in \mathbb{N}}$ of edge length maps converges for each interior edge e to a non-negative real number. In other words, $\lambda_n(e) \rightarrow \lambda_\infty(e) \in [0, \infty)$ for every $e \in E_{int}(T)$. Then, just as before, we define the limit to be the data $(T', i', V'_{col}, \lambda')$ given by

- (a) T' is the tree obtained from T by collapsing edges e for which $\lambda_\infty(e) = 0$. this defines a surjective morphism of bicolored based ribbon trees, $p : T \rightarrow T'$.
- (b) i' is the embedding obtained from i by contracting along collapsed edges.
- (c) $V'_{col} = p(V_{col})$
- (d) $\lambda'(e) = \lambda_\infty(p^{-1}(e))$, since every edge $e \in E_{int}(T')$ is the image of a unique edge in $E_{int}(T)$.

Proposition 2.3.3. $Gr(T, V_{col})$ is a polyhedral cone in \mathbb{R}^n , where $n = |E_{int}| - |V_{col}| + 1$.

Proof. There is an \mathbb{R}_+ action on $Gr(T, V_{col})$, given by $(\delta \cdot \lambda)(e) := \delta \lambda(e)$, so it is clearly a cone. The dimension follows from the fact that there are $|E_{int}|$ variables and $|V_{col}| - 1$ relations. The polyhedral structure can be seen by writing $|V_{col}| - 1$ variables as linear combinations of n independent variables. Then the condition that all $\lambda(e) \geq 0$ means that $Gr(T)$ is an intersection of half-spaces. \square

Example 2.3.4. In the example of Figure 27, $|E_{int}| = 8$, and $|V_{col}| = 5$. We can choose independent variables to be $\lambda_1, \lambda_2, \lambda_3, \lambda_8$, and express the remaining variables as

$$\begin{aligned} \lambda_4 &= \lambda_3 \\ \lambda_5 &= \lambda_3 \\ \lambda_6 &= \lambda_2 + \lambda_3 \\ \lambda_7 &= \lambda_1 + \lambda_2 + \lambda_3. \end{aligned}$$

Thus the space of admissible edge lengths is parametrized by points in the polyhedral cone that is the intersection of \mathbb{R}_+^4 (for the independent variables being non-negative) with the half-spaces $\lambda_4 \geq 0, \lambda_5 \geq 0, \lambda_6 \geq 0$ and $\lambda_7 \geq 0$.

Theorem 2.3.5. $Gr_{k,1}$ is homeomorphic to $M_{d,1}$, hence to \mathbb{R}^{k-1} .

Proof. We define a homeomorphism $\Theta : Gr_{k,1} \rightarrow M_{k,1}$.

Suppose first that the combinatorial type T has a single, bivalent, colored vertex. This is the case if and only if the colored vertex has the root on one side, and on the other side, the first vertex of valency at least 3, let's call it V . Set

$$z_0 = \infty, z_1 = 0, z_{i+1} - z_i = \prod_{e \in [e_i, V] \cap [e_{i+1}, V]} e^{-\lambda(e)}.$$

If $\lambda \geq 0$ is the edge length of the edge between the colored vertex and V , we set the horizontal line to be $\text{Im}(z) = e^\lambda$. For any other combinatorial type, we set

$$z_0 = \infty, z_1 = 0, z_{i+1} - z_i = \prod_{e \in [e_i, e_0] \cap [e_{i+1}, e_0]} e^{-\lambda(e)},$$

and the horizontal line to be

$$\text{Im}(z) = \prod_{e \in [v_{col}, e_0]} e^{-\lambda(e)},$$

which is independent of $v_{col} \in V_{col}$ because of the relations on the edge lengths. The

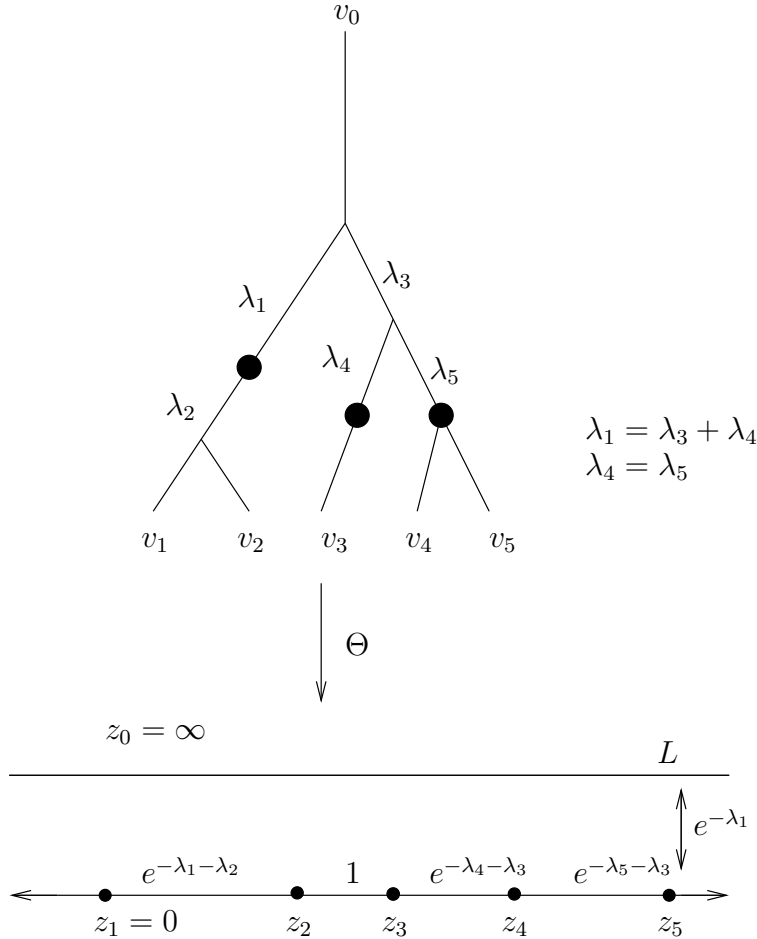


FIGURE 28. Identifying a bicolored metric ribbon tree in $Gr_{5,1}$ with a marked quilted disk in $M_{5,1}$.

continuity of Θ is clear, and injectivity and surjectivity follow as before.

□

Remark 2.3.6. As before one can think of Θ as identifying the polyhedral cones in $Gr_{d,1}$ with homeomorphic cones in \mathbb{R}^{d-1} in such a way that the boundaries match up as they should, and the union over the cones is \mathbb{R}^{d-1} .

Example 2.3.7. Consider the case $d = 3$, where we have fixed the parametrization of the elements of $M_{d,1}$ so that the height of the line L is 1. Let $x = z_2 - z_1$ and $y = z_3 - z_2$. The image of $\Theta : Gr_{3,1} \rightarrow M_{3,1}$ subdivides $\mathbb{R}_{>0}^2$ into 6 regions, see Figure 29, each of which corresponds to a cone in \mathbb{R}^2 via the homeomorphism $(x, y) \mapsto (\log x, \log y)$.

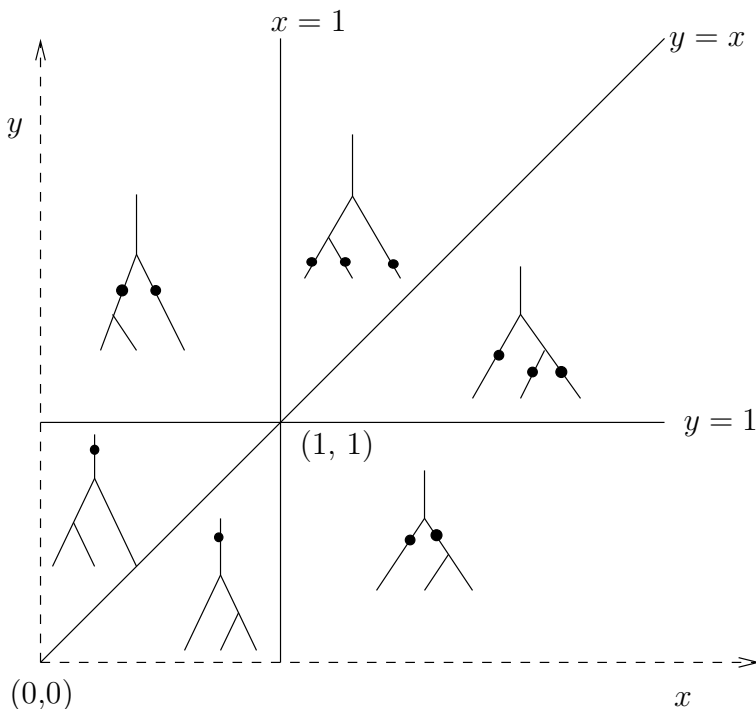


FIGURE 29. The image of the cones of $Gr_{3,1}$ in the moduli space $M_{3,1}$.

There is a natural compactification of $Gr_{d,1}$ by allowing edges to have length ∞ , and we denote this compactification by $\overline{Gr}_{d,1}$. The map Θ extends to the compactifications by taking limits in appropriate charts.

Proposition 2.3.8. $\Theta : \overline{Gr}_{d,1} \rightarrow \overline{M}_{d,1}$ is a homeomorphism.

Proof. It follows from the observation that if λ is the length of an edge in $Gr(T)$, then $e^{-\lambda}$ is the value of the ratio corresponding to that edge. Thus the image of a cone $Gr(T)$ is contained in the image of the ratio chart $M(T)$, and is identified directly with the subset of $M(T)$ for which all ratios in the chart are restricted to lie in the interval $(0, 1]$. This identification passes to the limits as λ approaches ∞ and the corresponding ratio approaches 0. This shows that Θ is a homeomorphism between $\overline{M}_{d,1}$ and $\overline{Gr}_{d,1}$. \square

2.4. TORIC VARIETIES AND MOMENT POLYTOPES.

We show that $\overline{M}_{d,1}$ can be identified with the non-negative part of an embedded toric variety in $\mathbb{C}P^k$, where k is the number of maximal bicolored trees with d leaves. Each such tree determines a monomial in the d variables $X_1, X_2, \dots, X_{d-1}, Y$. The weight vector of the monomial is read directly from the combinatorics of the tree. An immediate consequence is that $\overline{M}_{d,1}$ is homeomorphic to the moment polytope of the toric variety, which is the convex hull of the weight vectors.

Recall from Section 2.2.4 that a point in $M_{d,1}$ can be identified with a projective coordinate

$$\mathbf{X} = (X_1 : X_2 : \dots : X_{d-1} : Y),$$

by choosing a parametrization such that $z_0 = \infty$, and setting $X_i = z_{i+1} - z_i$ and Y to be the height of the line. To every maximal bicolored tree we associate a weight vector $\mathbf{N}_T \in \mathbb{Z}^d$, using an adaptation of the algorithm given by Forcey in [2].

Each pair of adjacent leaves in T , labelled i and $i+1$ say, determines a unique vertex, which we call v_i , in T . Let a_i be the number of leaves on the left side of v_i , and let b_i be the number of leaves on the right side of v_i . Let

$$\delta_i = \begin{cases} 0 & \text{if } v_i \text{ is below the level of the colored vertices, and} \\ 1 & \text{if } v_i \text{ is above the colored vertices.} \end{cases}$$

The weight vector is

$$\mathbf{N}_T = (a_1 b_1 (1 + \delta_1), \dots, a_i b_i (1 + \delta_i), \dots, a_{d-1} b_{d-1} (1 + \delta_{d-1}), - \sum_i \delta_i a_i b_i).$$

Example 2.4.1. For the tree pictured in Figure 30, the weight vector is $(2, 16, 6, 1, 4, -14)$, so the corresponding monomial is $X_1^2 X_2^{16} X_3^6 X_4 X_5^4 Y^{-14}$.

Remark 2.4.2. The convex hull realization of [2] is obtained from these weight vectors by projecting to the first $d-2$ coordinates. In other words, forgetting the exponents of the last variable Y (alternatively, setting $Y = 1$), is his construction for $q = 1/2$, scaled by a factor of 2.

Label the maximal bicolored trees T_1, \dots, T_k . We define a projective toric variety $V \subset \mathbb{C}P^{k-1}$ as the closure of the image of

$$(8) \quad (X_1 : \dots : X_{d-1}) \mapsto (\mathbf{X}^{\mathbf{N}_{T_1}} : \dots : \mathbf{X}^{\mathbf{N}_{T_k}}).$$

The entries in the weight vectors always sum to $d(d-1)/2$, so the monomials all have the same degree and the map is well-defined on the homogeneous coordinates.

Definition 2.4.3. For a maximal bicolored tree T , we can define a *flop* of an interior edge e as in Definition 1.4.2, as long as the edge e is incident to a pair of trivalent vertices. We define a *fusion* move through an interior vertex v_i to be the move by which

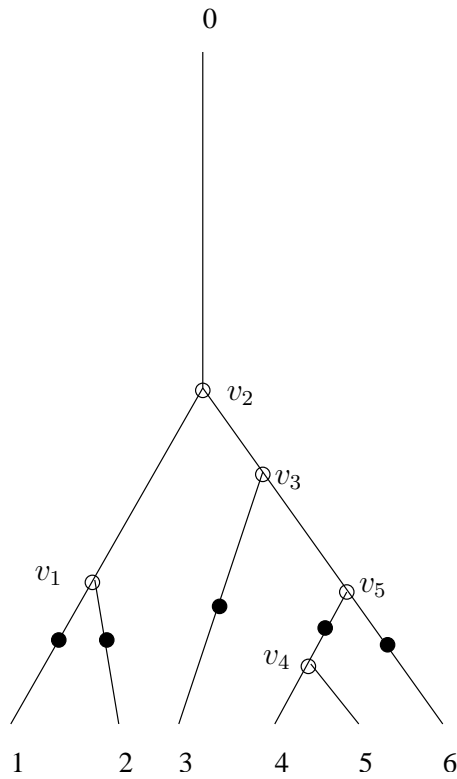


FIGURE 30. A maximal bicolored tree, whose weight vector is $(2, 16, 6, 1, 4, -14)$.

two colored vertices immediately below v_i become a single colored vertex immediately above v_i ; the vice-versa we will call a *splitting* move. We will say that two maximal bicolored trees T and T' differ by a *basic move* if they differ by a flop, fusion, or splitting move.

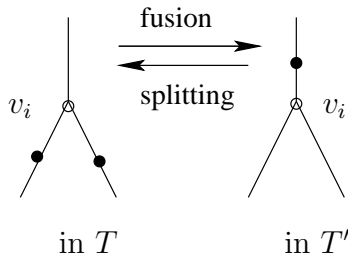


FIGURE 31. The other basic moves in a bicolored tree: fusion and splitting.

The important point is that any maximal bicolored tree can be obtained from any other such tree by a sequence of basic moves.

Lemma 2.4.4. *Suppose that two maximal bicolored trees T and T' differ by a single basic move involving an edge $e \in E(T)$. Let R denote the simple ratio labeling the edge e in the chart determined by T . Then*

$$\frac{\mathbf{X}^{\mathbf{N}_{T'}}}{\mathbf{N}_T} = R^m$$

for some integer $m > 0$. In general, for two trees T and T' ,

$$\frac{\mathbf{X}^{\mathbf{N}_{T'}}}{\mathbf{N}_T} = R_{i_1}^{m_1} R_{i_2}^{m_2} \dots R_{i_r}^{m_r}$$

for some ratios R_{i_1}, \dots, R_{i_r} in the ratio chart associated to T , and positive integers m_1, \dots, m_r .

Proof. Any maximal bicolored tree can be obtained from another by a sequence of basic moves. The first type, the flop, was dealt with in Lemma 1.4.3, and since the proof is practically the same we omit it here. For the other types of basic move, consider the situation in Figure 31, in which a colored vertex is below v_i in T , and above v_i in T' .

The weight vectors of T and T' are identical in all entries except for the i -th entry, which corresponds to the exponent of X_i , and the $n+1$ -th entry, which corresponds to the exponent of Y :

$$\begin{aligned} (\mathbf{N}_T)_i &= 2a_i b_i, \\ (\mathbf{N}_{T'})_i &= a_i b_i, \\ (\mathbf{N}_{T'})_{n+1} - (\mathbf{N}_T)_{n+1} &= -(0) - (-a_i b_i) \end{aligned}$$

Therefore

$$\begin{aligned} \frac{\mathbf{X}^{\mathbf{N}_{T'}}}{\mathbf{N}_T} &= \frac{X_i^{a_i b_i} Y^{-0}}{X_i^{2a_i b_i} Y^{-a_i b_i}} \\ &= \frac{Y^{a_i b_i}}{X_i^{a_i b_i}} \\ &= \left(\frac{Y}{X_i} \right)^{a_i b_i} \end{aligned}$$

where Y/X_i is the ratio labeling the two edges below v_i of T . The general case follows by induction on the number of basic moves. □

Theorem 2.4.5. $\overline{M}_{d,1}$ is homeomorphic to the non-negative part of the projective toric variety V .

Proof. The proof proceeds just like the proof of Theorem 1.4.4.

We show that each chart $M(T_i)$ is identified with the non-negative part of the affine slice $V \cap \mathbb{A}_i$, where

$$\mathbb{A}_i = (\xi_1 : \xi_2 : \dots : \underbrace{1}_{i^{\text{th}}} : \dots : \xi_k).$$

We prove it for the the first affine piece. $V \cap \mathbb{A}_1$ consists of all points

$$\left(1 : \frac{\mathbf{X}^{\mathbf{N}_{T_2}}}{\mathbf{X}^{\mathbf{N}_{T_1}}} : \dots : \frac{\mathbf{X}^{\mathbf{N}_{T_k}}}{\mathbf{X}^{\mathbf{N}_{T_1}}}\right)$$

where the ratios are allowed to be 0. Lemma 1.4.3 says that for any edge in T_1 , say with ratio R , there is an entry R^m in the slot belonging to the tree obtained by a flop of that edge. For any positive integer m , the map $r \mapsto r^m$ is a homeomorphism for $r \in [0, \infty)$, which is the domain of the ratios in the chart $M(T_1)$. The other entries are higher products of ratios in $M(T_1)$ so depend smoothly on the chart $M(T_1)$. Therefore $M(T_1)$ is homeomorphic to the non-negative part of $V \cap \mathbb{A}_1$. \square

Corollary 2.4.6. *$\overline{M}_{d,1}$ is homeomorphic to the convex hull of the weight vectors in \mathbb{R}^d , and is a $(d - 1)$ -dimensional polytope. It is also homeomorphic to the Stasheff multiplihedron J_d .*

Proof. The non-negative part of a projective toric variety constructed with weight vectors is homeomorphic, via the moment map, to the convex hull of the weight vectors (see, for example, [5], [11]). The proof that it is homeomorphic to the Stasheff multiplihedron K_d is by induction on d : the one-dimensional spaces $\overline{M}_{2,1}, \overline{M}_3, J_2$ and K_3 are all compact and connected, and so homeomorphic. It suffices, therefore, to show that $\overline{M}_{d,1}$ is the cone on its boundary. This is true since it is homeomorphic to a polytope. \square

Part 3. Stable scaled curves and morphisms of CohFT's

3.1. MODULI SPACE OF STABLE SCALED LINES.

In this section we re-interpret the moduli space of quilted disks as a *moduli space of stable scaled lines*. The same definition for the complex line will then define a complex algebraic variety that we will call the *complexified multiplihedron*, and denote by $\overline{M}_{n,1}^{\mathbb{C}}$. Geometrically, it arises naturally in Ziltener's study [14] of gauged pseudoholomorphic maps from the complex plane.

Definition 3.1.1. Let V be an affine line, with compactification $P = V \cup \{\infty\}$ the projective line. A *scaled marked line* is a datum (V, z, ϕ) , where V is isomorphic to the affine line, $z = (z_1, \dots, z_n) \in V$ are distinct points, and $\phi : TV \rightarrow V$ is a translationally invariant volume form on V .

Remark 3.1.2. The map $\phi \mapsto \phi(x, 1) \in V$, for $x \in V, 1 \in T_x V$ uniquely identifies a translationally invariant volume form ϕ with an element $v_\phi \in V \setminus \{0\}$. An affine transformation $\psi : V \rightarrow V$ is of the form $x \mapsto ax + b$, for some $a \neq 0, b \in V$, and such a transformation induces a map $\Psi : TV \rightarrow TV$ given by $\Psi(x, \xi) = (\psi(x), \psi_*\xi) = (\psi(x), a\xi)$. Since

$$\begin{aligned} v_{\Psi^*\phi} &:= (\Psi^*\phi)(x, 1) \\ &= \Phi(\psi(x), \psi_*1) \\ &= \Phi(x, a) \\ &= a\Phi(x, 1) \\ &= av_\phi, \end{aligned}$$

we see that the element v_ϕ scales under such transformations in the same way as a vector field; thus v_ϕ can be alternatively interpreted as a translationally invariant vector field v_ϕ on V , acted on by affine transformations $\psi(x) = ax + b$ via the usual push-forward $\psi_*v_\phi = av_\phi$.

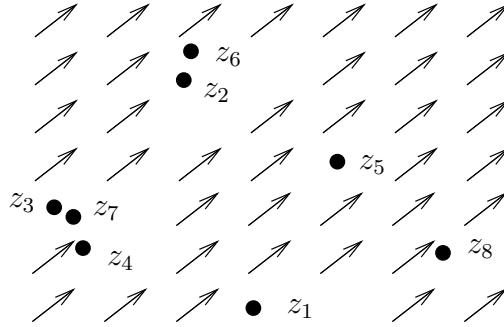


FIGURE 32. A configuration in $M_{8,1}(\mathbb{C})$, of 8 marked points $z_1, \dots, z_8 \in \mathbb{C}$ and a translationally invariant vector field v . A distinguished marked point z_0 is identified with ∞ .

Definition 3.1.3. An *isomorphism of scaled marked lines* is a morphism $\psi : V \rightarrow V$ that preserves the volume form. A scaled line is *stable* if the automorphism group is finite, that is, has at least one marking. Denote by $M_{n,1}(C)$ the corresponding moduli space of stable, scaled marked lines.

Remark 3.1.4. In the case $C = \mathbb{R}$, $M_{n,1}(\mathbb{R}) = M_{n,1}$ of the previous section, through identifying (z_1, \dots, z_n, ϕ) with $(z_0 = \infty, z_1, \dots, z_n, L_\phi)$, where L_ϕ is a line of height v_ϕ .

$M_{n,1}(C)$ has a natural compactification, obtained by allowing the points to come together and the volume form ϕ to scale. For any nodal curve \tilde{C} with markings z_0, \dots, z_n , we distinguish a special point w_i of \tilde{C}_i by taking it to be the marking z_0 , and otherwise the node closest to z_0 .

Definition 3.1.5. A (*genus zero*) *nodal scaled marked line* is a datum (\tilde{C}, z, ϕ) , where \tilde{C} is a (genus zero) nodal curve, $z = (z_0, \dots, z_n)$ is a collection of markings disjoint from the nodes, and for each component \tilde{C}_i of \tilde{C} , the line $C_i := \tilde{C}_i \setminus \{w_i\}$ is equipped with a (possibly zero or infinite) translationally invariant volume form ϕ_i . We call a volume form ϕ_i *degenerate* if it is zero or infinite.

An automorphism of a stable nodal scaled curve is an automorphism of the nodal curve preserving the volume forms and the markings. A nodal scaled marked curve is *stable* if it has finite automorphism group, or equivalently, if each component with non-degenerate (resp. degenerate) volume form has at least two (resp. three) special points. We follow Ziltener's convention of drawing the components with non-degenerate components with a singularity at the root, reflecting the singularity of the volume form there. The darkly resp. medium resp. lightly shaded regions have zero resp. finite resp. infinite volume form.

The combinatorial type of a point in $\overline{M}_{n,1}(C)$ is a rooted bicolored tree, just as with the moduli space of quilted disks; vertices represent components of the nodal curve, edges represent nodes, labeled semi-infinite edges represent the markings, with the root always labelled by z_0 . Every path from a leaf back to the root must pass through exactly one colored vertex. The vertices lying between the root and the colored vertices correspond to darkly shaded regions, the colored vertices themselves correspond to medium shaded regions, and the rest correspond to lightly shaded regions, See Figure 33 for an example of a stable marked scaled curve and its combinatorial type.

Now we specialize to the case $C = \mathbb{C}$. Let $\overline{M}_{n,1}^{\mathbb{C}} := \overline{M}_{n,1}(\mathbb{C})$ denote the moduli space of isomorphism classes of stable scaled marked (complex) curves. $M_{n,1}^{\mathbb{C}}$ contains as a subspace those scaled marked curves such that all markings lie on the projective real line, $\mathbb{R}P := \mathbb{R} \cup \{\infty\}$; these are naturally identified with marked disks. More accurately, $M_{n,1}^{\mathbb{C}}$ admits an antiholomorphic involution induced by the antiholomorphic involution of P , such that $M_{n,1} = M_{n,1}(\mathbb{R})$ is the subset of the fixed point set such that the points are in the given order. The involution extends to an antiholomorphic involution of $\overline{M}_{n,1}^{\mathbb{C}}$. The multiplihedron $\overline{M}_{n,1}$ can be identified with the subset of the fixed point set such that the points are in the required order.

3.1.1. Charts with cross-ratios. We can use cross-ratios as coordinates on $M_{n,1}^{\mathbb{C}}$ in the same way as we did for $M_{n,1}$. A point in $M_{n,1}^{\mathbb{C}}$ is an equivalence class of the data $\{z_1, \dots, z_d, v_\phi\}$, to which we add a distinguished point $z_0 = \infty$. Define two types of coordinates, of the form ρ_{ijkl} where i, j, k, l are distinct indices in $0, 1, \dots, d$, and of the form $\rho_{i,j}$, where i, j are distinct indices in $1, \dots, d$. The ρ_{ijkl} are defined as before, and the $\rho_{i,j}$ are defined as follows: given a representative $\{z_1, z_2, \dots, z_d, v\}$, let $\psi_{ij} : \mathbb{C} \rightarrow \mathbb{C}$

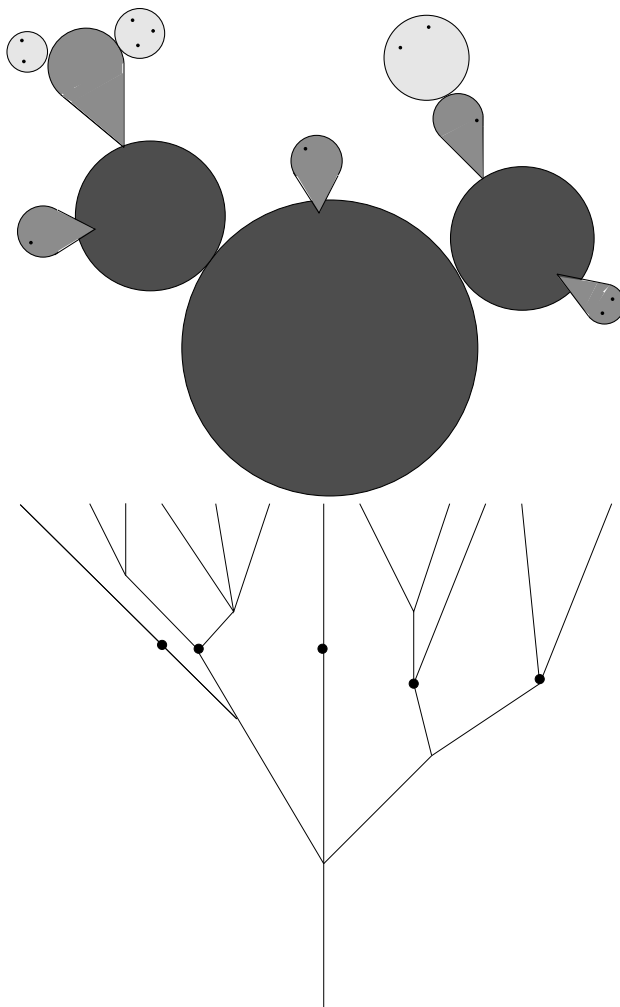


FIGURE 33. Stable marked scaled curve and its combinatorial type.

be the (unique) affine transformation that maps z_i to 0 and z_j to 1. Then

$$\begin{aligned} \rho_{ij}([z_1, \dots, z_d, v]) &:= (\psi_{ij})_* v \\ &= \frac{1}{z_j - z_i} v. \end{aligned}$$

The coordinates extend to the compactification $\overline{M}_{n,1}^{\mathbb{C}}$. For the coordinates ρ_{ijkl} , choose a component in the bubble tree for which at least three of the markings representing

z_i, z_j, z_k and z_l are distinct, and set

$$\rho_{ijkl} = \begin{cases} \infty, & \text{if } z_i = z_j \text{ or } z_k = z_l, \\ 1, & \text{if } z_i = z_k \text{ or } z_j = z_l, \\ 0, & \text{if } z_i = z_l \text{ or } z_j = z_k. \end{cases}$$

For the coordinates $\rho_{i,j}$, let α denote the unique bubble at which z_0, z_i and z_j are distinct. Then

$$\rho_{i,j} = \begin{cases} 0, & \text{if } \alpha \text{ is darkly shaded,} \\ \infty, & \text{if } \alpha \text{ is lightly shaded.} \end{cases}$$

The properties **(Invariance)**, **(Symmetry)**, **(Recursion)** and **(Relations)** hold as before for ρ_{ijkl} and $\rho_{i,j}$, and extend to the compactification $\overline{M}_{n,1}^{\mathbb{C}}$ already described. Given the combinatorial type of a stable scaled curve, one can choose a local chart of cross-ratios according to the same prescription as given in Section 2.2.3. The cross-ratios in the chart can also be chosen such that the Recursion relations among the cross-ratios for the edges satisfy the condition that for all paths from a colored vertex to the root, the products of the cross-ratios along those edges are the same. Such relations are toric, so $\overline{M}_{n,1}^{\mathbb{C}}$ has at worst toric singularities.

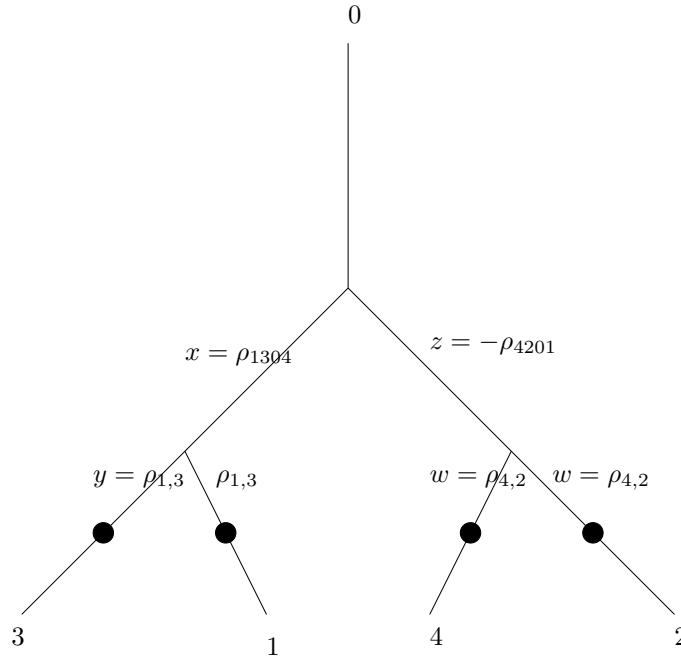


FIGURE 34. A cross-ratio chart in $\overline{M}_{4,1}^{\mathbb{C}}$. The relation is $xy = zw$, which gives a toric singularity.

The boundary structure of $\overline{M}_{n,1}^{\mathbb{C}}$ is similar to that of $\overline{M}_{n,1}$. First, for any $I \subset \{1, \dots, n\}$ we have a divisor $\iota_I : D_I \rightarrow \overline{M}_{n,1}^{\mathbb{C}}$ corresponding to the formation of a single bubble containing the markings I . We have a homeomorphism

$$(9) \quad D_I \cong \overline{DM}_{0,|I|+1} \times \overline{M}_{n-|I|+1,1}^{\mathbb{C}}$$

where $\overline{DM}_{0,n}$ denotes the Deligne-Mumford space of stable, n -pointed curves of genus zero.

Second, for any partition $I_1 \cup \dots \cup I_r$ of $\{1, \dots, n\}$ we have a divisor $D_{I_1 \cup \dots \cup I_r}$ corresponding to the formation of r bubbles with markings I_1, \dots, I_r , attached to a remaining component with infinite volume form. We have a homeomorphism

$$(10) \quad D_{I_1 \cup \dots \cup I_r} \cong \prod_{i=1}^r \overline{M}_{|I_i|+1,1}^{\mathbb{C}} \times \overline{DM}_{0,r}.$$

3.2. MORPHISMS OF COHOMOLOGICAL FIELD THEORIES

The complexified multiplihedron leads naturally to a notion of morphism of cohomological field theories. Recall that the boundary of the Deligne-Mumford moduli space $\overline{DM}_{g,n}$ of isomorphism classes of stable curves of genus g with n markings consists of the following divisors:

- (a) a divisor $\iota_{g-1,n+2} : D_{g-1,n} \rightarrow \overline{DM}_{g,n}$ corresponding to the formation of a non-separating node, isomorphic to $\overline{DM}_{g-1,n+2}$. The inclusion is obtained by identifying the last two marked points.
- (b) for each splitting $g = g_1 + g_2$, $\{1, \dots, n\} = I_1 \cup I_2$ a divisor $\iota_{g_1+g_2, I_1 \cup I_2} : D_{g_1+g_2, I_1 \cup I_2} \rightarrow \overline{DM}_{g,n}$ corresponding to the formation of a separating node, splitting the surface into pieces of genus g_1, g_2 with markings I_1, I_2 . The divisor $D_{g_1+g_2, I_1 \cup I_2}$ is isomorphic to $\overline{DM}_{g_1, |I_1|+1} \times \overline{DM}_{g_2, |I_2|+1}$, except in the cases $I_1 = I_2 = \emptyset$ and $g_1 = g_2$ in which case there is an additional automorphism.

Definition 3.2.1. (Kontsevich-Manin) An (even) cohomological field theory (CohFT) with values in a ring R is a free R -module V of finite rank equipped with a non-degenerate inner product and a collection of *correlators*

$$V^n \times H^\bullet(\overline{DM}_{g,n}, \mathbb{Q}) \rightarrow R, \quad (\alpha, \beta) \mapsto \langle \alpha; \beta \rangle_{g,n}$$

satisfying the following two splitting axioms:

$$\begin{aligned} \langle \alpha; \beta \wedge \gamma_{g-1,n+2} \rangle_{g,n} &= \sum_k \langle \alpha, \delta_k, \delta^k; \iota_{g-1,n+2}^* \beta \rangle_{g-1,n+2} \\ \langle \alpha; \beta \wedge \gamma_{g_1+g_2, I_1 \cup I_2} \rangle_{g,n} &= \sum_k \langle \alpha_{I_1}, \delta_k; \cdot \rangle_{g_1, |I_1|+1} \langle \alpha_{I_2}, \delta^k; \cdot \rangle_{g_2, |I_2|+1} (\iota_{g_1+g_2, I_1 \cup I_2}^* \beta) \end{aligned}$$

where δ_k is a basis for V , δ^k is a dual basis, the dots indicate insertion of the Kunneth components of $\iota_{g_1+g_2, I_1 \cup I_2}^* \beta$, and γ denotes the dual classes to the divisor D . (There is an additional factor of 2 in the exceptional case $g_1 = g_2$, $I_1 = I_2 = \emptyset$ arising from the additional automorphism.)

By duality, any set of correlators determine maps

$$\mu^{g,n} : V^n \times H^\bullet(\overline{DM}_{g,n+1}, \mathbb{Q}) \rightarrow V, \quad \langle \mu^n(\alpha_1, \dots, \alpha_n; \beta), \alpha_0 \rangle = \langle \alpha_0, \dots, \alpha_n; \beta \rangle_{g,n+1}$$

which are the complex analogs of the A_∞ -structure maps. The various relations on the divisors in $\overline{DM}_{g,n}$ give rise to relations on the maps $\mu^{g,n}$. In particular the relation

$$[D_{0, \{0,3\} \cup \{1,2\}}] = [D_{0, \{0,1\} \cup \{2,3\}}]$$

in $H^2(\overline{DM}_{0,4}, \mathbb{Q})$ implies that $\mu^{0,2} : V^2 \rightarrow V$ is associative.

To define morphism of cohomological field theory, we first have to deal with the problem that $\overline{M}_{n,1}^{\mathbb{C}}$ is not smooth, and so not every Weil divisor admits a dual class. That is, for a Weil divisor

$$(11) \quad D = \sum_I n_I [D_I] + \sum_{I_1 \cup \dots \cup I_r} n_{I_1 \cup \dots \cup I_r} [D_{I_1 \cup \dots \cup I_r}]$$

there may or may not exist a class $\gamma \in H^2(\overline{M}_{n,1}^{\mathbb{C}}, \mathbb{Q})$ that satisfies

$$\langle \beta, [D] \rangle = \langle \beta \wedge \gamma, [\overline{M}_{n,1}^{\mathbb{C}}] \rangle, \quad \beta \in H^\bullet(\overline{M}_{n,1}^{\mathbb{C}}).$$

Let V and W be cohomological field theories.

Definition 3.2.2. A *morphism of cohomological field theories* is a collection of maps

$$\phi^n : V^n \times H^\bullet(\overline{M}_{n,1}^{\mathbb{C}}, \mathbb{Q}) \rightarrow W$$

such that for any divisor D of the form (11) with dual class $\gamma \in H^2(\overline{M}_{n,1}^{\mathbb{C}}, \mathbb{Q})$ we have

$$(12) \quad \begin{aligned} \phi^n(\alpha, \beta \wedge \gamma) &= \sum_I n_I \phi^{n-|I|+1}(\mu_V^{|I|}(\alpha_i, i \in I; \cdot), \alpha_j, j \notin I; \cdot)(\iota_I^* \beta) \\ &\quad + n_{I_1 \cup \dots \cup I_r} \mu_W^r(\phi^{|I_1|}(\alpha_i, i \in I_1; \cdot), \dots, \phi^{|I_r|}(\alpha_i, i \in I_r; \cdot); \cdot)(\iota_{I_1 \cup \dots \cup I_r}^* \beta) \end{aligned}$$

where \cdot indicates insertion of the Kunneth components of $\iota_I^* \beta$, $\iota_{I_1 \cup \dots \cup I_r}^* \beta$, using the homeomorphisms (9), (10).

In particular, the equivalence

$$[D_{\{1,2\}}] = [D_{\{1\}, \{2\}}]$$

in $H^2(\overline{M}_{2,1}^{\mathbb{C}}, \mathbb{Q}) = \mathbb{Q}$ implies that $\phi^1 : V \rightarrow W$ is a homomorphism,

$$\phi^1 \circ \mu_V^2 = \mu_W^2 \circ (\phi^1 \times \phi^1).$$

Ezra Getzler has proposed another definition of weak morphism of cohomological field theories, via equivalence with Frobenius manifolds. Elsewhere we plan to give examples of morphisms of cohomological field theories arising from Gromov-Witten theory, and discuss composition of morphisms of cohomological field theories.

REFERENCES

- [1] J. M. Boardman and R. M. Vogt. *Homotopy invariant algebraic structures on topological spaces*. Springer-Verlag, Berlin, 1973. Lecture Notes in Mathematics, Vol. 347.
- [2] Stefan Forsey. Convex hull realizations of the multiplihedra. arXiv:math.AT/0706.3226.
- [3] K. Fukaya, Y.-G Oh, H. Ohta and K. Ono. Lagrangian intersection Floer theory: anomaly and obstruction. in preparation, preliminary version available at <http://www.kusm.kyoto-u.ac.jp/~fukaya/fooo.dvi>.
- [4] Kenji Fukaya and Yong-Geun Oh. Zero-loop open strings in the cotangent bundle and Morse homotopy. *Asian J. Math.*, 1(1):96–180, 1997.
- [5] William Fulton. *Introduction to toric varieties*, volume 131 of *Annals of Mathematics Studies*. Princeton University Press, Princeton, NJ, 1993. , The William H. Roever Lectures in Geometry.
- [6] Norio Iwase and Mamoru Mimura. Higher homotopy associativity. In *Algebraic topology (Arcata, CA, 1986)*, volume 1370 of *Lecture Notes in Math.*, pages 193–220. Springer, Berlin, 1989.
- [7] M. Kontsevich and Yu. Manin. Gromov-Witten classes, quantum cohomology, and enumerative geometry [MR1291244 (95i:14049)]. In *Mirror symmetry, II*, volume 1 of *AMS/IP Stud. Adv. Math.*, pages 607–653. Amer. Math. Soc., Providence, RI, 1997.
- [8] Jean-Louis Loday. Realization of the Stasheff polytope. *Arch. Math. (Basel)*, 83(3):267–278, 2004.
- [9] Dusa McDuff and Dietmar Salamon. *J-holomorphic curves and symplectic topology*, volume 52 of *American Mathematical Society Colloquium Publications*. American Mathematical Society, Providence, RI, 2004.
- [10] David Nadler and Eric Zaslow. Constructible sheaves and the Fukaya category. arXiv:math.SG/0604379.
- [11] Frank Sottile. Toric ideals, real toric varieties, and the moment map. In *Topics in algebraic geometry and geometric modeling*, volume 334 of *Contemp. Math.*, pages 225–240. Amer. Math. Soc., Providence, RI, 2003.
- [12] James Stasheff. *H-spaces from a homotopy point of view*. Lecture Notes in Mathematics, Vol. 161. Springer-Verlag, Berlin, 1970.
- [13] James Dillon Stasheff. Homotopy associativity of H -spaces. I, II. *Trans. Amer. Math. Soc.* 108 (1963), 275-292; *ibid.*, 108:293–312, 1963.
- [14] F. Ziltener. *Symplectic vortices on the complex plane and quantum cohomology*. PhD thesis, Zurich, 2006.